Hsp90 mediates temperature regulation on the Arabidopsis circadian clock

Dissertation

zur

Erlangung des Doktorgrades (Dr. rer. nat.)

der

Mathematisch-Naturwissenschaftlichen Fakultät

der

Rheinische Friedrich-Wilhelms-Universität Bonn

vorgelegt von

Zisong Ma

aus

Suzhou, China

Bonn 2014

Die vorliegende Arbeit am Max-Planck Institut für Pflanzenzüchtungsforschung Köln, in der Arbeitsgruppe von Prof. Dr. Seth J. Davis, Abteilung für Entwicklungsbiologie der Planzen (Direktor Prof. Dr. George Coupland) angefertigt.

1. Prof. Dr. Seth J. Davis
2. Prof. Dr. Dorothea Bartels

Tag der Promotion: 04.06.2014
Erscheinungsjahr: 2014

Abstract

To anticipate rhythmic changes and optimize timing of physiological events, many organisms have evolved an internal-timing mechanism named the circadian clock. In Arabidopsis, its clock system consists of the positive/negative feedback loops, which are formed by oscillating components. The internal circadian rhythm resonates with daily environmental changes. The circadian clock can be set by two major exogenous cues: light and temperature. The clock components CCA1, LHY, PRR7, PRR9, TOC1, GI, and ELF3 are involved in the temperature regulation on the circadian clock, but the detailed mechanism, for how their inputs are processed still remains poorly understood. Hsp90 is one of the most important protein chaperons in living organisms. Hsp90 is intensively involved in the heat-stress response. Therefore, I proposed that Hsp90 participates in clock regulation in *Arabidopsis*.

In Chapter 3, Hsp90 was genetically and pharmacologically proved to influence the circadian clock. The period length was lengthened in the *hsp90.2-3* mutant. Moreover, the phase response assay showed that Hsp90.2 particularly influenced the circadian clock before dawn. A chemical-epitasis assay on clock mutants revealed that CCA1 and LHY were involved in the Hsp90 regulation pathway. Interestingly, I found that the period length was closely related to the transcription patterns of *CCA1* and *LHY*. Furthermore, by using the qRT-PCR approach, I found that *PRR9* which represses the transcription of *CCA1* was also involved in the Hsp90 regulation pathway. ELF3 was demonstrated to be the transcription repressor of *PRR9* and the repression is altered by temperature particularly in the dark. This is consistent with the result of my phase response assay. In microscope assay, I found that Hsp90.2 transferred into the nucleus and co-localized with ELF3. Afterwards, an *in vivo* protein binding assay showed the interaction between Hsp90.2 and ELF3. Together, I could connect Hsp90.2 to an input at an oscillator component.

In Chapter 4, I examined the clock phenotypes of other *hsp90.2* mutants after entrainment to either light or temperature. The *hsp90.2-6* and *hsp90.2-7* mutation resulted in a longer period under LD conditions whereas *hsp90.2-4* and *hsp90.2-8* resulted in a shorter period under WC conditions. Together, allele specific effects were detected.

Taken together, my thesis has placed Hsp90 within the clock input pathway. CCA1, LHY, PRR9 and ELF3 were all identified as targets in Hsp90 regulation pathway. Since different *hsp90.2* mutations caused different clock phenotype, therefore I propose that more than one input pathways are thought to be present in Arabidopsis.

Zusammenfassung

Um rhythmische Veränderungen zu antizipieren und zeitliche Abläufe physiologischer Ereignisse zu optimieren, haben viele Organismen einen internen Zeitmechanismus entwickelt, der „circadian clock“ (tagesrhythmische Uhr) genannt wird. Das Uhrsystem von Arabidopsis besteht aus positiv/negativ Rückkopplungsschleifen, die von oszillierenden Komponenten gebildet werden. Der interne zyklische Rhythmus schwingt mit täglichen Veränderungen der Umgebung. Die „circadian clock“ kann von zwei externen Hauptsignalen eingestellt werden: Licht und Temperatur. Die Uhrkomponenten CCA1, LHY, PRR7, PRR9, TOC1, GI, und ELF3 sind in die Temperaturregulation der „circadian clock“ involviert, aber der detaillierte Mechanismus darüber, wie die Beiträge dieser verarbeitet werden, ist weiterhin wenig verstanden. Hsp90 ist eines der wichtigsten Proteinchaperone lebender Organismen. Hsp90 ist stark in die Hitzestressreaktion involviert. Daher stelle ich die These auf, dass Hsp90 an der Regulation der „circadian clock“ in *Arabidopsis* partizipiert.

In Kapitel 3 wurde genetisch und pharmakologisch bewiesen, dass Hsp90 die „circadian clock“ beeinflusst. Die Periode der Uhr war in der *hsp90.2-3* Mutante verlängert. Weiterhin wurde durch ein Phasenreaktionstest gezeigt, dass Hsp90.2 die „circadian clock“ vor Sonnenaufgang teilweise beeinflusste. Eine chemische Epitasisuntersuchung an Uhrmutanten deckte auf, dass CCA1 und LHY in den Hsp90 Regulationsweg involviert waren. Von starkem Interesse war mein Befund, dass die Länge der Periode eng mit den Transkriptionsmustern von *CCA1* und *LHY* verwandt war. Weiterhin fand ich, durch den Einsatz von qRT-PCR, heraus, dass *PRR9*, welches die Transkription von *CCA1* reprimiert, auch in den Regulationsweg von Hsp90 involviert war. ELF3 war als Transkriptionsrepressor von *PRR9* vorgestellt worden und die Repression ist im Dunkeln temperaturabhängig. Dies stimmt mit den Ergebnissen meine Phasenreaktionstests überein. Über Mikroskopie fand ich heraus, dass Hsp90.2 in den Nukleus transferiert wurde und dort mit ELF3 kolokalisierte. Danach zeigte ein *in vivo* Proteinbindungsversuch die Interaktion zwischen Hsp90.2 und ELF3. Zusammenfassend konnte ich Hsp90.2 mit einem Beitrag zu einem Oszillatorkomponenten verbinden.

In Kapitel 4 untersuchte ich die Phänotypen anderer *hsp90.2* Mutanten in Bezug auf die Uhr, nachdem diese entweder durch Licht oder Temperatur konditioniert wurden. Die *hsp90.2-6* und *hsp90.2-7* Mutationen resultierten in längeren Perioden in LD Bedingungen, während *hsp90.2-4* and *hsp90.2-8* in WC Bedingungen kürzere Perioden zeigten. Zusammenfassend wurden allelspezifische Effekte detektiert.

Insgesamt konnte Hsp90 durch meine Thesis im Inputnetzwerk der Uhr platziert werden. CCA1, LHY, PRR9 und ELF3 wurden jeweils als Ziele des Regulationsweges von Hsp90 identifiziert. Da unterschiedliche hsp90.2 Mutationen unterschiedliche „circadian clock“ Phänotypen nach sich zogen, stelle ich die These auf, dass mehr als ein Weg für Inputs in Arabidopsis existiert.

Table of Contents

List of figure elements

List of tables

Abbreviations

CAB	CHLOROPHYLL A/B BINDING PROTEIN
CCA1	CIRCADIAN CLOCK ASSOCIATED 1
CCG	Clock-control gene
CCR2	COLD AND CLOCK REGULATED 2
DD	constant darkness
EC	evening complex
EE	Evening Element
ELF3	EARLY FLOWERING 3
ELF4	EARLY FLOWERING 4
FT	FLOWERING LOCUS T
GA	gibberellic acid
GDA	geldanamycin
GFP	green fluorescent protein
GI	GIGANTEA
HSE	heat shock element
HSF	heat shock factors
HSP	heat shock protein
LD	light/dark
LHCB	*LIGHT-HARVESTING CHLOROPHYII A/B-BINDING PROTEIN*
LHY	LATE AND LONG HYPOCOTYL
LOV	Light, Oxygen, or Voltage
LUC	LUCIFERASE
LUX	LUX ARRYTHMO
NB-LRR	nucleotide-binding site and leucine-rich repeat
PIF4	PHYTOCHROME INTERACTING FACTOR 4
PRR	PSEUDO RESPONSE REGULATOR
RFP	red fluorescent protein
TAA1	TRYPTOPHAN AMINOSTRANSFERASE OF ARABIDOPSIS 1
TOC1	TIME OF CAB EXPRESSION
WC	warm/cool

ZT	zeitgeber time
ZTL	ZEITLUPE

Chapter 1 Introduction

1.1 Introduction to circadian rhythms

The Earth's rotation constantly generates the rhythmic changes of environment conditions. The most obvious diurnal changes are light and temperature. As a consequence, many organisms have evolved an internal-timing mechanism to anticipate those rhythmic changes. This internal-timing mechanism is the called circadian clock. Circadian rhythms are endogenously generated by the circadian clock. To match the daily alternation, most organisms have an approximate 24-hour circadian clock, which drives sleeping and awaking, mental concentration, hormone levels, and body-temperature homeostasis. (Dunlap *et al.*, 2004). The circadian clock also regulates processes that occur seasonally, including flowering in plants, hibernation in mammals, and long-distance migration in butterflies (Harmer, 2009). In Arabidopsis, the circadian clock regulates approximately one-third of genes and 36% of Arabidopsis promoters are circadian regulated (Covington *et al*., 2008; Michael and McClung, 2003).

Plants were the first organisms for which the observation of circadian rhythms was noted. The discovery and research on the circadian clock dates back to the fourth century B.C. Androsthenes discovered that tamarind opened and closed their leaves rhythmically over the course of 24 hours (Bretzl, 1903). The first experiment for circadian rhythm was performed in 18th century by a French astronomer, de Mairan. From his work on leaf movement of plants kept in the dark, he concluded that there was an internal-timing mechanism involved in growth (de Mairan J, 1729). The molecular study of plant clocks began in 1985 with the observation that mRNA abundance of the *LIGHT-HARVESTING CHLOROPHYII A/B-BINDING PROTEIN* (*LHCB*) of peas oscillated with a circadian rhythm (Kloppstech, 1985). In addition to plants, chronobiology studies were performed in many diverse organisms, such as cyanobacteria, fungi, yeast, insects and mammals. (Dunlap *et al.*, 2004)

The internal circadian clock is reset by exogenous cues daily to keep synchronized with the diurnal circle. This process is called entrainment and such exogenous cues are often referred to as "*zeitgebers*" (or "time-givers"). For most organisms, the dominant *zeitgebers* are light and temperature signals. Light input to the clock occurs via multiple types of photoreceptors. For example, in plants the

phytochrome and cryptochrome photoreceptors control red and blue light signaling to the clock (Devlin and Kay, 2000; Somers *et al*., 1998a). Light regulation of the circadian clock occurs within multiple loops of the circadian clock at transcriptional, posttranscriptional, and posttranslational levels (Kim *et al*., 2007; Lidder *et al*., 2005; Yakir *et al*., 2007). For temperature, however, the input and regulation pathway remains poorly understood. Entrainment is mediated by clock-input pathways. The central clock is likely composed of multiple interlocked feedback loops, clock outputs may also be directly regulated by clock input signaling pathways, and clock components may act both within the central clock and in input and output signaling pathways (Harmer, 2009).

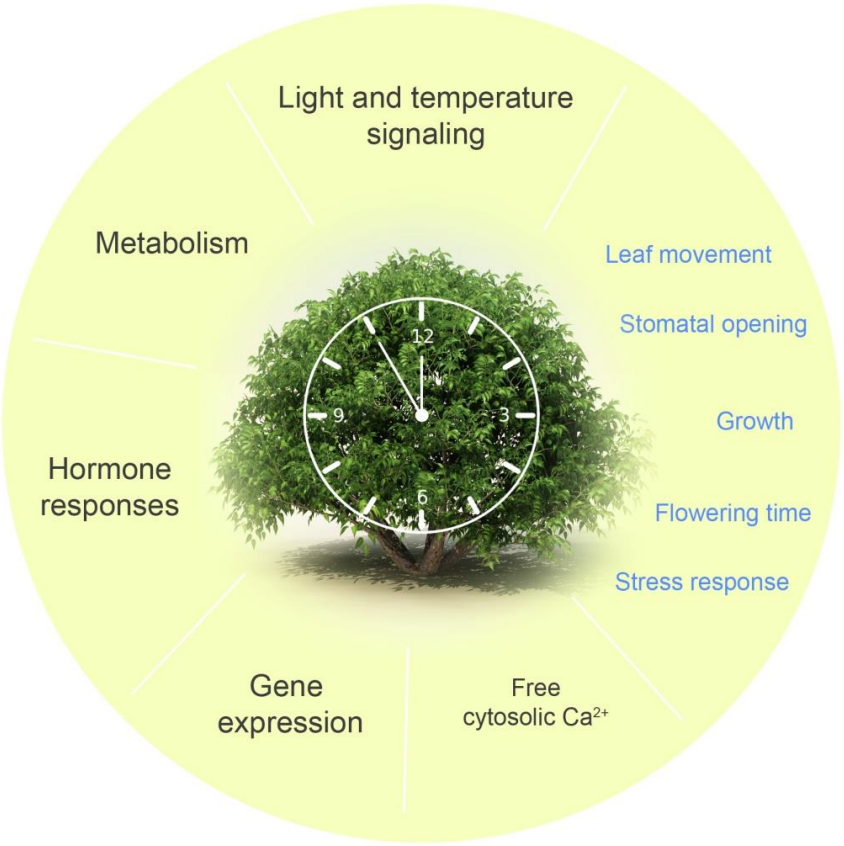

Figure 1.1 The plant circadian clock system.

Many physiological processes are regulated by the circadian clock through the output pathways (black and blue items). Moreover, the clock is reset by the input pathways (black items). Simultaneously, the input pathways are circadian regulated through the output pathways.

Cyanobacteria and higher plants gain an advantage when the endogenous

period is matched to the external diurnal cycle (Highkin and Hanson, 1954; Ouyang *et al*., 1998; Woelfle *et al*., 2004), which is named fitness advantage. Plants with a clock period matched to the environment contain more chlorophyll, fix more carbon, grow faster, and survive better than plants with circadian periods differing from their environment (Dodd *et al*., 2005).

1.2 The Arabidopsis circadian clock

1.2.1Tools to investigate clock function

Circadian rhythms can be mathematically described in the form of sinusoidal waves. The rhythm wave includes three main properties: period, phase, and amplitude (Figure 1.2). Period is the time length of one cycle and defines the speed of the circadian rhythm. Phase describes the timing of specific events within the circadian day. Amplitude is defined as half of the difference between the maximum and the minimum value of an oscillation. Additionally, the accuracy of circadian oscillation is described by its robustness. The lack of circadian rhythms being sustainable is defined as arrhythmicity. By circadian convention, the time of onset of a signal that resets the clock is defined as *zeitgeber* (“time-giver”) time 0, abbreviated ZT0. ZT0–ZT12 represents the “day”, the time when the organism was exposed to light, whereas ZT12–ZT24 represents “night”. (Harmer, 2009). Similarly, the organisms are in warmth during ZT0-ZT12, and in coolness during ZT12-24.

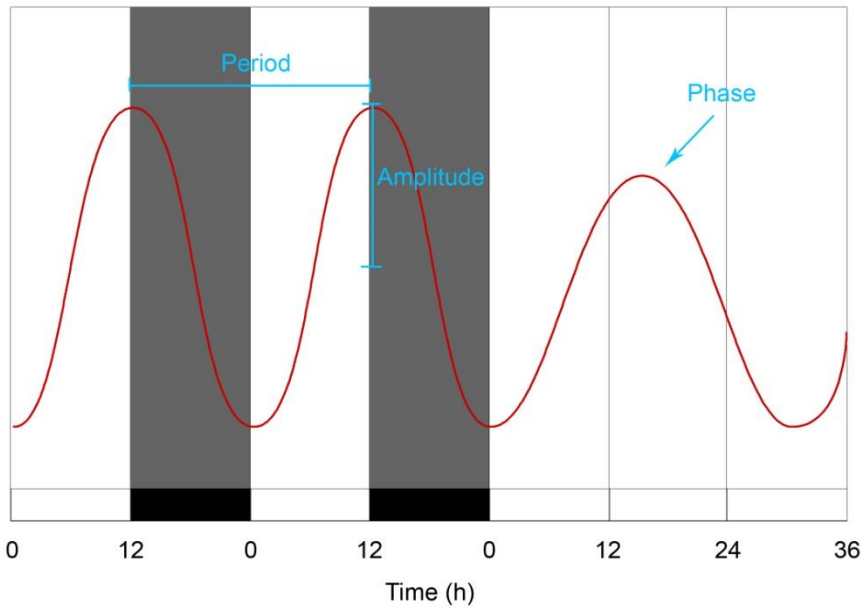

Figure 1.2 Analysis of circadian rhythms.

The figure shows the main features of bioluminescence-based circadian experiments. Period is the time length of one cycle and defines the speed of the circadian rhythm. Phase refers to the timing of

specific events within the circadian day. Amplitude is half the difference between the maximum and the minimum value of an oscillation.

To monitor the plant circadian rhythm and investigate the mechanism underlying the circadian clock, various approaches have been established during the past centuries. The most obvious daily rhythm is that of leaf movement. Plant leaves change the position and leaf-angle state during a day. By monitoring leaf movement, it was found that in a free-running condition, plants have a non-24-hour periodicity (de Mairan J, 1729). Monitoring flowering time of plants led to the insights of the seasonal regulation of circadian clock (McClung, 2006). Many other bioprocesses such as growth, photosynthesis, state of stomata, are also recognized as being clock regulated (Yakir *et al*., 2007).

In the early 90s, a reporter gene, firefly luciferase expressed under the control of a clock-regulated gene, provided a visual output of the endogenous rhythm. This boosted circadian research in Arabidopsis (Millar *et al*., 1992). The luciferase gene was fused to the promoter of a clock-regulated gene. Subsequently, in the presence of luciferin, the luciferase substrate, bioluminencense emission by the luciferase closely tracked the activity of the promoter driving its expression. Among the commonly monitored clock-controlled genes, *CHLOROPHYLL A/B BINDING PROTEIN (CAB)* was the first luciferase-fused reporter (*CAB::LUC*) to be used for clock study (Millar *et al*., 1995). Because the dampening of *CAB* expression in the dark limits the use of *CAB::LUC* for DD (constant darkness) experiments, the *COLD AND CIRCADIAN REGULATED* (*CCR2*) was accepted as an ideal substitute, which can also maintain its robust rhythm under DD condition (Covington *et al*., 2001; Hanano *et al*., 2006; Heintzen *et al*., 1997; McWatters *et al*., 2007; Schoning *et al*., 2007). So far, the promoters of core-clock components, such as *CCA1*, *LHY*, *TOC1*, *GI*, *PRR7*, and *PRR9*, have been commonly fused with luciferase gene, serving as indicators of clock rhythm at different peak times. During the past years, luciferase-based visualization assay in Arabidopsis has been a powerful tool for the discovery of clock traits (Martin-Tryon *et al*., 2007; Millar *et al*., 1995; Onai *et al*., 2004; Somers *et al*., 2000; Strayer *et al*., 2000).

Other assays also contribute to the study of clock function. Quantitative reverse

transcriptase–polymerase chain reaction (qRT-PCR) assays allow quantifying the rhythmic expression of genes in diverse genetic backgrounds. DNA microarrays allow surveying genome-wide circadian regulation of gene expression, leading to important insights into clock function (Covington and Harmer, 2007; Covington *et al*., 2008; Edwards *et al*., 2006; Harmer *et al*., 2000; Michael *et al*., 2008; Schaffer *et al*., 2001). Taken together, these molecular-level assays have led to recent rapid progress in the plant circadian clock research field.

1.2.2 The circadian clock model

The mathematic model of the plant circadian clock consists of three interlocked transcriptional feedback loops: the core loop, the morning loop and the evening loop (Figure 1.3). The core loop consists of three components: *CIRCADIAN CLOCK ASSOCIATED 1* (*CCA1*), *LATE ELONGATED HYPOCOTYL* (*LHY*) and *TIME OF CAB EXPRESSION 1* (*TOC1*). Both *CCA1* and *LHY* are morning-phased Myb-related transcription factors (Romero *et al*., 1998), while *TOC1*, also known as *PSEUDO-RESPONSE REGULATOR 1* (*PRR1*), one of the pseudo-response regulator family members, is an evening-phased, clock-regulated gene. CCA1 and LHY bind directly to the *TOC1* promoter and inhibit its expression during the day (Alabadi *et al*., 2001). However, TOC1 also represses transcription of *CCA1* and *LHY* at night. In the absence of the core loop, the circadian clock stays arrhythmic, which suggests that CCA1, LHY, and TOC1 are notably important for the circadian clock in Arabidopsis. CCA1 and LHY are partially genetically redundant. The loss of *CCA1* or *LHY* results in a shorter clock period (Green and Tobin, 1999; Mizoguchi *et al*., 2002). However, overexpression of either *CCA1* or *LHY* causes arrhythmicity of the clock (Schaffer *et al*., 1998; Wang and Tobin, 1998). Overexpression of *CCA1* or *LHY* can generate a long-hypocotyl and late-flowering phenotype. Similar with *CCA1* and *LHY*, the loss of *TOC1* results in a shorter period (Mas *et al*., 2003a; Millar *et al*., 1995; Somers *et al*., 1998b). The *TOC1* promoter contains the evening element (EE), whose sequence is AAATATCT (Harmer *et al*., 2000). The EE was found in many clock-regulated genes showing a peak at dusk and was necessary for proper circadian expression (Harmer *et al*., 2000). CCA1 and LHY bind to the EE of the

TOC1 promoter to repress the transcription of *TOC1* (Alabadi *et al*., 2001; Harmer *et al*., 2000).

The morning loop is formed by *CCA1*, *LHY*, *PRR7*, and *PRR9*. Besides *TOC1* (*PRR1*), the *PRR* family contains the other four members: *PRR3*, *PRR5*, *PRR7*, and *PRR9*. Reverse-genetic studies revealed that these *PRR* genes all play a role in the plant clock (Eriksson *et al*., 2003; Farre *et al*., 2005; Kaczorowski and Quail, 2003; Michael *et al*., 2003; Nakamichi *et al*., 2005; Salome and McClung, 2005). During the day, PRR9 and PRR7 bind to the promoter of *CCA1* and *LHY* to repress their transcription (Nakamichi *et al*., 2010; Nakamichi *et al*., 2005). Reciprocally, LHY and CCA1 induce the expression of *PRR9* and *PRR7* by direct binding to their promoter (Farre *et al*., 2005; Portoles and Mas, 2010). The *prr7*, *prr9*, and the double mutant *prr7 prr9*, all display long-period phenotypes (Alabadi *et al*., 2001; Farre *et al*., 2005; Yamamoto *et al*., 2003), while the *prr5 prr7 prr9* triple mutant is essentially arrhythmic (Nakamichi *et al*., 2005).

Mathematical modeling suggests there is an evening loop comprising TOC1 and an unknown component Y. Y positively regulates *TOC1* expression and the expression of Y is predicted to be negatively regulated by TOC1 (Locke *et al*., 2005). Partial Y function was assigned to the evening gene *GIGANTEA* (*GI*). Both GI mRNA and protein are clock regulated, with peaks around dusk. The timing of *GI* accumulation would be consistent with *TOC1* (Alabadi *et al*., 2001). However, high levels of *TOC1* found in the *gi* mutants suggested additional components may assist in Y function (Martin-Tryon *et al*., 2007).

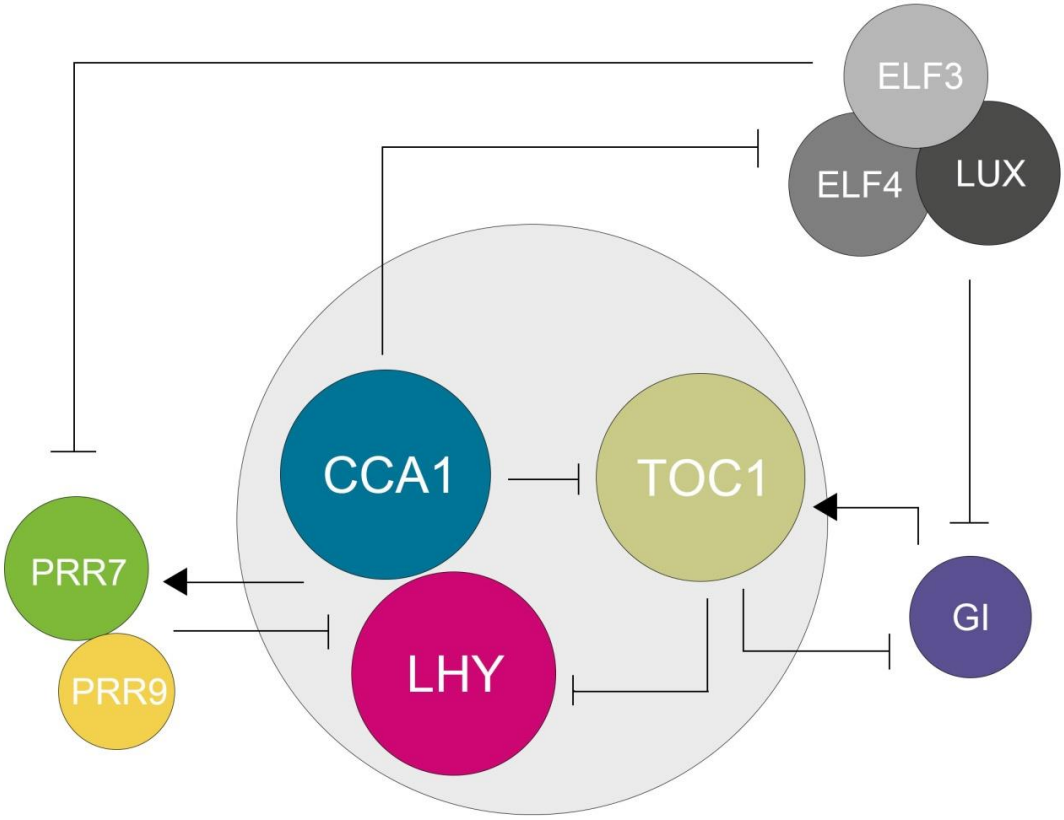

Figure 1.3 One Arabidopsis circadian clock model.

Circadian-clock components are arranged in interlocked feedback loops. In the core loop, CCA1 and LHY negatively regulate *TOC1* expression whereas TOC1 represses *CCA1* and *LHY*. In the morning loop, PRR7 and PRR9 negatively regulate *LHY* and *CCA1* whereas CCA1 and LHY induce *PRR7* and *PRR9*. In the evening loop, TOC1 represses *GI* expression, whereas GI activates *TOC1* expression. In addition, CCA1 and LHY represses *ELF3*, *ELF4*, and *LUX* expression. LUX, ELF3, and ELF4 form a evening complex and repress *PRR7*, *PRR9*, and *GI* expression.

In addition to transcriptional regulation, posttranscriptional process also plays a critical role in proper clock functions. The stability and translation of some mRNAs are influenced by the circadian clock and light signaling (Gutierrez *et al*., 2002; Kim *et al*., 2003; Lidder *et al*., 2005), and the abundance of many clock proteins is under posttranslational control. For example, ZTL, an F-box protein, interacts with both TOC1 and PRR5, leading to their degradation by the 26S-proteasome (Baudry *et al*., 2010; Kiba *et al*., 2007; Mas *et al*., 2003b). ZTL protein interactions are mediated by the LOV (Light, Oxygen, or Voltage) domain that also functions as a blue-light photoreceptor. The blue light stimulates the physical interaction between GI and ZTL.

This interaction stabilizes both ZTL and GI (David *et al*., 2006; Fujiwara *et al*., 2008; Kiba *et al*., 2007; Kim *et al*., 2007; Mas *et al*., 2003b).

1.3 Temperature sensing and signalling in plants

Plants are exposed to daily and seasonal fluctuations in temperature. As an environmental variable, temperature limits the distribution and induces the variation of plants on the earth, partially due to strong influence on plant development by non-stress temperatures.

1.3.1 Temperature affects plant development

Within the non-stress range of 12–27°C, plants dramatically differ in growth rates and developmental responses (Samach and Wigge, 2005). Lower temperature slows down growth. This is generally due to reduced enzymatic activities and biochemical reactions (McClung and Davis, 2010). However, mutations in growth repressor gene DELLA in gibberellic acid (GA) signaling, are able to compromise the inhibition effect of low temperature (Kumar *et al*., 2012; Stavang *et al*., 2009). As one thermal response, hypocotyl lengthening helps Arabidopsis to adapt to hotter conditions (Crawford *et al*., 2012; van Zanten *et al*., 2009). Temperature controls hypocotyl elongation through a regulator *PHYTOCHROME INTERACTING FACTOR 4* (*PIF4*) (Proveniers and van Zanten, 2013). The *pif4* mutants are unable to increase hypocotyl length at warmer temperatures (Koini *et al*., 2009; Stavang *et al*., 2009).

The flowering of plant is also strongly affected by temperature (Kumar and Wigge, 2010). Warm temperature induction of flowering in Arabidopsis is triggered by an upregulation in the expression of the floral integrator gene *FLOWERING LOCUS T* (*FT*) (Balasubramanian *et al*., 2006). A class of micro- RNAs (miRNAs) responsive to ambient temperature mediates the temperature regulation on flowering timing. Changes in the ambient temperature range lead to alterations in steadystate miRNA abundance. Furthermore, with the overexpression of miR172, expression of *FT* ignores higher temperature and increases. On the other hand, the acceleration of flowering in response to a high temperature requires the activity of PIF4 (Proveniers and van Zanten, 2013). *FT* expression regulated by PIF4 binding to its promoter is highly temperature-dependent (Kumar *et al*., 2012).

1.3.2 Hormones signaling pathway is temperature-dependent

Plant hormones play a major role in both cell division and cell expansion. As a key hormonal factor, auxin can facilitate both division and elongation (Mockaitis and Estelle, 2008), which are sensitive to the changes of ambient temperature. PIF4 is also involved in the auxin signalling pathway in response to higher temperature. PIF4 increases auxin biosynthesis in response to higher temperatures by binding to promoters of three auxin biosynthesis genes, *TRYPTOPHAN AMINOSTRANSFERASE OF ARABIDOPSIS 1* (*TAA1*), *CYTOCHROME P450*, *FAMILY 79, SUBFAMILY B*, *PEPTIDE 2* (*CYP79B2*) and *YUCCA8*, and subsequently upregulating their expresssion (Franklin *et al*., 2011; Hornitschek *et al*., 2012; Sun *et al*., 2012).

1.3.3 Circadian clock is temperature-regulated

Two major influences of temperature on the circadian clock are entrainment and compensation. Entrainment of the circadian clock, primarily via the detection of changes in light and temperature, maintains synchronization between the surrounding environment and the endogenous clock mechanism. In Arabidopsis, thermocycles are able to entrain the clock in constant light. A key player necessary for thermal entrainment is the evening loop component *EARLY FLOWERING3* (*ELF3*), as *elf3* mutants are unable to entrain in thermocycles in darkness (Thines and Harmon, 2010). Circadian clocks are able to maintain robust rhythms that are constant over a broad range of physiological temperatures. This property is termed temperature compensation. A dynamic balance between LHY and GI functions maintains robust and accurate rhythmicity at higher temperatures, while at lower temperatures, CCA1 plays a greater role than LHY in temperature compensation (Gould *et al*., 2006). Thermocycles also act on a number of processes such as cell cycle, protein synthesis and DNA replication independently of photocycles, suggesting that different sensory mechanisms are involved in transmitting temperature information to the clock (Michael *et al*., 2008). Enrainment and compensation are described in further details below.

1.4 Temperature regulation on circadian clock

1.4.1 Temperature entrainment

Acting as a *zeitgeber*, temperature can set the phase of the clock. This process is termed temperature entrainment. It appears that temperature and light entrainments are two partially independent processes, as nonoverlapping QTL for the two entrainment conditions exists (Boikoglou et al., 2011).

PRR7 and PRR9 are demonstrated as the key components in temperature entrainment. The *prr7-3* mutant display a long period for *CCA1*, *LHY* and *TOC1* and the *prr9-1* mutant exhibit a long period phenotype as well. The *prr7-3 prr9-1* double mutant displays a much longer period (>32 h), compared to either single mutant, indicating that PRR7 and PRR9 are partially functionally overlapped. The *prr7-3 prr9-1* mutant is compromised in its ability to entrain to thermocycles. When transferred from photocycles to thermocycles, the *prr7-3 prr9-1* seedlings fail to maintain the 24h period and even becomes arrhythmic under some conditions, indicating an inability to entrain. Additionally, when exclusively entrained to thermocycles, the *prr7-3 prr9-1* double mutant is seen to be arrhythmic either during or after entrainment. However, the entrainment defect is rescued when the *prr7-3 prr9-1* mutant is entrained to higher-temperature (28°C /22°C) thermocycles. Furthermore, the *prr7-3 prr9-1* double mutant is not able to be reset by temperature pulses (Salome and McClung, 2005; Salome et al., 2010). Taken together, PRR7 and PRR9 are required for temperature to set the clock.

ELF3 is also involved in the temperature entrainment. The *elf3* mutant is unable to maintain rhythmicity following 4°C or 10°C thermocycle differences (McWatters et al., 2000; Thines and Harmon, 2010). The temperature induction of *PRR7*, *PRR9*, and *GI* mRNA accumulations are eliminated in the *elf3-1* mutant. However, the basal accumulation levels of these genes are elevated, especially at night. In contrast, overexpression of ELF3 does not affect the phase response to temperature, which indicates that ELF3 is a target of temperature input, but not a perceiver of temperature (Thines and Harmon, 2010).

1.4.2 Temperature compensation

Plants are naturally exposed to fluctuations of ambient temperature. However, the circadian clock can maintain robust and accurate rhythms over a broad range of physiological temperatures, which is termed temperature compensation.

In Arabidopsis, the morning loop components CCA1, LHY, PRR7, and PRR9 play an important role in the temperature-compensation mechanism. The *prr7 prr9* mutant maintains the same period length as wild type at 12°C, but is lengthened at higher temperatures, demonstrating overcompensation (Salome et al., 2010). Temperature compensation is restored when expression of CCA1 and LHY are reduced, demonstrating that temperature compensation through PRR7 and PRR9 at high temperature is completely CCA1-/LHY-dependent (Salome et al., 2010). Furthermore, reduction of CCA1 and LHY expression in wild type and *prr7 prr9* resulted in a short period at all temperatures, suggesting that PRR7 and PRR9 are regulated by CCA1 and LHY in the temperature compensation mechanism (Salome et al., 2010).

In addition to CCA1 and LHY, GI is also involved in the temperature-compensation mechanism (Gould et al., 2006). The *GI* gene encodes a 127-kD nuclear protein. *GI* is regulated by the circadian clock, with a peak in expression 12 h after dawn (Fowler et al., 1999). In addition to its role in flowering, GI was also identified to affect the circadian clock, as the *gi* mutant cause a short-period phenotype (Park et al., 1999). Meanwhile, the *gi* mutation results in a reduction in the expression of *CCA1* and *LHY* (Fowler et al., 1999). The *gi* mutant shows normal period phenotypes at low temperatures, but becomes sensitive to high temperatures, suggesting that the existence of GI expands the temperature range, over which the circadian rhythm can remain robust and accurate. It has been demonstrated that GI maintains robustness and accuracy of the circadian clock at higher temperatures by the temperature-dependent regulation of *TOC1*, thereby maintaining expression of *CCA1* and *LHY* to sustain clock functions. A dynamic balance between LHY and GI functions at higher temperature partially explains the temperature compensation mechanism. At lower temperatures, CCA1 plays a greater role than LHY in

temperature compensation and the maintenance of rhythm robustness (Gould et al., 2006).

1.5 Hsp90 and plant circadian clock

1.5.1 Molecular chaperones and heat stress

Molecular chaperones are families of proteins that assist the folding of newly synthesized or misfolded proteins, prevent protein aggregation and protect subunits from stresses during the assembly of complexes (Saibil, 2013). Their increased expression in response to stress is a key characteristic for cell self-protection. Most of the main chaperones work in the ATP-dependent way, facilitating their folding or unfolding (Mayer, 2010), particularly in response to thermal changes in protein folding.

Organisms are sometimes exposed to various stressful conditions, including sudden temperature increases. Proteins and cell structures are evolutionarily optimized to be only stable at certain temperatures. Even a small increase in temperature can cause protein unfolding, degradation, and unspecific aggregation. In response to heat stress, organisms have evolved a protection mechanism leading to the transient expression of heat shock proteins (Hsps). The increased levels of Hsps in response to moderate stress conditions are the basis for this resistance (Lindquist, 1986). Hsps are located in the cytoplasm under normal physiological conditions. However, under stress conditions, some of these Hsps rapidly transfer to the nucleus (Horwitz, 1992; Lindquist and Craig, 1988). Interestingly, increased Hsps due to one type of stress provide protection against other stresses, which is termed ‘‘crossprotection’’ (Lindquist, 1986).

Based on molecular mass, Hsps are divided into five major and conserved families—Hsp60s, Hsp70s, Hsp90s, Hsp100s (the number indicates the molecular mass of each HSP subunit), and small heat shock proteins (sHsps). Hsp60 acts at early stages of folding whereas Hsp90 acts at a late stage of folding of substrates, integrating signaling functions. Hsp70 directs substrates for unfolding, disaggregation, refolding or degradation. Hsp100 cooperates with either a protease ring for degradation or Hsp70 for disaggregation, avoiding the toxic effects of aggregation. Hsp70 and Hsp90 are highly interactive, functioning with many partners and cofactors. The domains of Hsp70 and Hsp90 interact with specific co-chaperones, which regulate their functions in a variety of ways.

1.5.2 Heat shock protein 90

Heat shock protein 90 (Hsp90) is a highly conserved and abundant (i.e., ~1% of total proteins) protein in prokaryotic and eukaryotic cells, involved in the assembly, maturation, stabilization and activation of key signaling proteins and in assisting cell survival under stresses (Pearl and Prodromou, 2006; Picard, 2002).

In animals, Hsp90 mediates extensive signal transduction, including assisting folding of steroid hormone receptors, protein kinases, and transcription factors, as well as activation of the substrate to initiate stress signal transduction (Jackson et al., 2004; Shinozaki et al., 2006; Wegele et al., 2004; Zuehlke and Johnson, 2010). Hsp90 is involved in controlling normal growth of human cell and in promoting tumor cell development (Scroggins et al., 2007; Zuehlke and Johnson, 2010). So far, a number of Hsp90 genes have been identified from many plants. It was recently shown that Hsp90s play an important role in plant development, stress response, and disease resistance (Jarosz and Lindquist, 2010; Rizhsky et al., 2002; Sangster and Queitsch, 2005).

Hsp90 is a flexible dimer with intrinsic ATPase activity. Almost all homologs of Hsp90 are conserved, containing three domains: an N-terminal conserved ATP-binding domain, a middle domain, and a C-terminal dimerization domain (Cowen, 2008; Terasawa et al., 2005; Wayne et al., 2011; Young et al., 2001). The N-terminal ATP-binding domain contains the ATP/ADP binding site. ATP binding and hydrolysis causes the conformational alteration of the N-terminal domain (Hessling et al., 2009; Mickler et al., 2009). Some natural substances, such as GDA, closely bind to this position to interfere with Hsp90 functions (Whitesell et al., 1992). The middle domain plays a key role in binding to substrate. The C-terminal domain is necessary for dimerization, and it also serve as the binding site of calmodulin and other substrates (Jackson et al., 2004).

In Arabidopsis, several isoforms of Hsp90 have been found. Among these isoforms, Hsp90.1, Hsp90.2, Hsp90.3, and Hsp90.4 are identified to be located in the cytoplasm. Hsp90.5, Hsp90.6, and Hsp90.7 were predicted to be located within the plastidial, mitochondrial, and endoplasmic reticulum, respectively (Milioni and Hatzopoulos, 1997; Sangster and Queitsch, 2005). Hsp90.2, Hsp90.3, and Hsp90.4

have high similarity, which suggests that they are functionally redundant. Loss of Hsp90 function in plants resulted in abnormal plant phenotypes, including an epinastic cotyledon, disc or radial symmetry of cotyledons, and abnormal growth of root hairs (Queitsch et al., 2002). It has been demonstrated that Hsp90 participated in the seed embryo formation and seed germination and Hsp90 also affected elongation of the hypocotyl (Prasinos et al., 2005; Sangster et al., 2008b).

Hsp90 can be induced by both abiotic and biotic stresses in plants. One of the typical abiotic stresses is heat shock stress. Hsp90 is known to be involved in regulation of heat shock response. In the promoters of Hsps, there are several heat shock elements (HSEs) which can be bound by heat shock factors (HSFs). Under normal conditions, Hsp90.2 negatively regulates transcription of heat-induced genes by suppression of HSF. Under heat shock stress, Hsp90.2 is inactivated while HSF is activated to induce expression of genes containing HSF elements (Yamada et al., 2007). Under stress conditions, the HSFs closely integrate with HSE to initiate transcription of Hsp genes (Jarosz and Lindquist, 2010; Lohmann et al., 2004). In addition, it was identified that overexpression of Hsp90.2 suppresses *HsfA2* transcription whereas HsfA2 is induced under inhibition of Hsp90.2 (Nishizawa-Yokoi et al., 2010). In response of biotic stress, Hsp90 mediates signaling pathways of disease resistance in plants. Plant immunity is initiated by resistance (R) proteins which provide disease resistance specificity by conferring resistance to pathogen strains expressing the certain molecule. The largest class of R protein contains a nucleotide-binding site and leucine-rich repeats, which are termed NB-LRRs (Sangster et al., 2008a). The interactions of Hsp90 and SGT1 (suppressor of the G2 allele of skp1) and RAR1 (required for Mla12 resistance) stabilize NLR (nucleotide-binding domain and LRR) proteins, which mediate plant defense mechanisms (Shirasu and Schulze-Lefert, 2003). Disease resistance mediated by RPM1, an NB-LRR protein, was weakened in *hsp90.2* mutant plants (Hubert et al., 2003).

1.5.3 Hsp90 and the clock

As described above, Hsp90 can assist the assembly, maturation, stabilization of signaling proteins and it has a broad range of client proteins in Arabidopsis. Interestingly, a number of the cytosolic Hsp90 genes oscillate with an evening phase

under light-dark cycles. Recent studies showed that inhibition of cytoplasmic Hsp90 by Hsp90-specific inhibitor GDA and RNAi-mediated depletion results in a long-period phenotype. Meanwhile, it was proposed that the clock component ZEITLUPE (ZTL) is the client of Hsp90, which suggests that Hsp90 is involved in the clock regulation pathway. *in vitro* “holdase” assay showed that Hsp90 associates with ZTL, protecting ZTL against denaturation. Furthermore, the gene expression of *TOC1* and *PRR5* was found to be altered when Hsp90 is depleted, which is subsequently thought to be mediated by ZTL. As the stabilizer of ZTL, neither of the mRNA and protein levels of GI is affected by inhibition of Hsp90. However, GI was demonstrated to be linked with Hsp90 in the posttranslational regulation of ZTL (Kim et al., 2011). So far, how Hsp90 regulates the circadian clock in Arabidopsis still remains poorly understood and further studies are needed for the detailed mechanism.

1.6 Thesis objectives

Previous studies have shown that temperature is an important external cue to influence the plant circadian clock through two processes named entrainment and compensation. It has been demonstrated that PRR7, PRR9 and ELF3 are the key components involved in the temperature entrainment process. The *prr7-3 prr9-1* mutant is not able to be entrained to normal temperature cycles (Salome and McClung, 2005). Similarly, the *elf3* mutant shows arrhythmicity following 4°C or 10°C thermocycle differences (McWatters et al., 2000; Thines and Harmon, 2010). Temperature compensation is a collaboration work of CCA1, LHY, PRR7, PRR9, and GI. Temperature compensation through PRR7 and PRR9 at high temperature is completely CCA1-/LHY-dependent (Salome et al., 2010). However, GI also maintains robustness and accuracy of the circadian clock at higher temperatures by maintaining expression of *CCA1* and *LHY* to sustain the clock function (Gould et al., 2006). In addition, Hsp90 has been shown to influence the circadian clock through ZTL (Kim et al., 2011).

My PhD thesis aimed to identify the role of Hsp90 in temperature regulation on the circadian clock. As Hsp90 is a chaperon protein responding to temperature change and stress, it is highly likely that Hsp90 serves as a temperature sensor and mediates the temperature signaling. For this, I examined the alteration of clock phenotypes by both mutating Hsp90.2 and inhibiting Hsp90 protein with its specific inhibitor, GDA. To identify the detailed molecular pathway, I tested if the gene expression of clock components are affected by Hsp90.2 under temperature conditions. Finally, I examined the interaction between Hsp90.2 and its potential targets. Further, I examined the other *hsp90.2* mutants to see how their circadian clock behaves.

Chapter 2 Material and methods

2.1 Materials

2.1.1 Mutant lines

Table 2.1 Mutant and transgenic lines previously made

Mutant and transgenic lines previously made	Background	Reference
hsp90.2-1	Col	David A. Hubert, 2003
hsp90.2-3	Col	David A. Hubert, 2003
hsp90.2-4	Col	David A. Hubert, 2003
hsp90.2-6	Col	David A. Hubert, 2003
hsp90.2-7	Col	David A. Hubert, 2003
hsp90.2-8	Col	David A. Hubert, 2003
PRR7::PRR7-GFP	Col	Nakamichi N, 2010
PRR9::PRR9-GFP	Col	Nakamichi N, 2010
prr7-3	Col	Salome and McClung, 2005
prr9-1	Col	Salome and McClung, 2005
prr7-3 prr9-1	Col	Salome and McClung, 2005

Table 2.2 Luciferase lines

LUC marker	Background	Selection marker
CCR2:LUC	Ws-2	Hygromycin
CCA1:LUC	Col	PPT
LHY:LUC	Col	Hygromycin
GI:LUC	Col	PTT
TOC1:LUC	Col	PTT
hsp90.2-1 GI:LUC	Col	PTT
hsp90.2-3CCR2:LUC	Ws-2	Hygromycin
hsp90.2-4 GI:LUC	Col	PTT
hsp90.2-6 GI:LUC	Col	PTT
hsp90.2-7 GI:LUC	Col	PTT
hsp90.2-8 GI:LUC	Col	PTT
prr7 LHY:LUC	Col	Hygromycin
prr9 LHY:LUC	Col	Hygromycin
prr7 GI:LUC	Col	PTT
prr9 GI:LUC	Col	PTT
cca1 CCR2:LUC	Ws-2	Hygromycin
lhy CCR2:LUC	Ws-2	Hygromycin
cca11 lhy CCR2:LUC	Ws-2	Hygromycin
toc1 CCR2:LUC	Ws-2	Hygromycin

2.1.2 Chemicals

1,4 Dithiothreitol (DTT) (biomol, #04010.5)

2-(N-morpholino)ethanesulfonic acid, MES (Duchefa, #M1503)

3′,5′-Dimethoxy-4′-hydroxyacetophenone, Acetosyringone (Sigma, # D134406)

Acrylamide (29:1) (Roth, #A124.1)

Adenine hemisulfate (Sigma, #A-9126)

Agarose (Bio-Budget, #10-35-1020)

Ammonium persulfate (Sigma, #A7460)

Bactoagar (BD, #214040)

Bacto-tryptone (BD, #211705)

Beef extract (BD, #212303)

Boric acid (Merck, #1.00165)

Bromophenol blue (Sigma, #47522)

Carbenicillin (Sigma, #C-1389)

Chloramphenicol (Sigma, #C-0378)

Chloroform (Merck, #1.02445)

cOmplete® EDTA-free tablets (Roche, #11873580001)

cOmplete® Mini EDTA-free tablets (Roche, #11836170001)

Dimethyl sulfoxide, DMSO (J.T. Baker, #7157)

DL-Phosphinothricin, PPT (Duchefa, #P0159)

D-Luciferin (Synchem, #S039)

Ethanol (J.T.Baker, #8006)

Ethidium bromide (Sigma; #46067)

Ethylenediaminetetraacetic acid, EDTA (Merck, #944)

GDA (Sigma, #G3381)

Gentamicin sulfate (Sigma, #G-3632)

GFP-Trap (ChromoTek, #110714001A)

Glutathione sepharose 4B (GE Healthcare Life Sciences, #17-0756-01)

Glycerol (Roth, #7530.1)

Glycine (Roth, #3908.2)

Hygromycin (Duchefa, #H0192)

Imidazole (Sigma, #56750)

IPTG (Roth, #2316.2)

Isopropanol (Appli. Chem., #A0900)

Kanamycin sulfate (Duchefa, #K4378)

KLORIX®, commercial sodium hypochlorite solution

Lithium Acetate (Sigma, #L-5750)

Lithium chloride (Li Cl) (Roth, #3739.1)

Magnesium chloride (Roth, #KK36.3)

Methanol (Chem Solute, #1437.2511)

Murashige and Skoog media, MS (Sigma, #M5524 and Duchefa, #M0221)

Na_2HPO_4 (Sigma, #S0876)

NaH_2PO_4 (Merck, #1.06346)

Ni-NTA Agarose (Qiagen, #139298931)

Peptone (Difco, #0122-17-4)

Phenol /Chloroform (Roth, #A156.1)

Phytoagar (Duchefa, #P0001)

Protease Inhibitors Cocktail for plant cell and tissue extracts (Sigma, #P9599)

Rifampicin (Sigma, #83907)

Sodium Acetate (Merck, #1.06268)

Sodium chloride, NaCl (Mecrk, #1.37017)

Sodium deoxycholate (Fluka, #30970)

Sodium dodecyl sulfate, SDS (Roth, #23.26.2)

Spectinomycin (Sigma, #S-9007)

Streptomycin (Sigma, #S-9137)

Sucrose (Roth, #4621)

Tetramethylethylenediamine (TEMED) (Fluka, #87689)

Tris (hydroxymethyl) aminomethane Hydrochloride, Tris HCl (Roth, #5429.3)

Triton-X100 (Roth, #3051)

Urea (Sigma, #33247)

Yeast extract (BD, #212750)

2.1.3 Reagents for each method

Seed sterilization

Bleach solution: 33% KLORIX® (v/v)
0.01% agar in sterile ddH_2O (w/v)

Growth media for plants

Table 2.3 MS media for plants

MS1	MS1 (3% agar)	MS3
4.4 g/L MS 0.5 g/L MES 10 g/L Sucrose 1.5% Phytoagar pH 5.7	4.4 g/L MS 0.5 g/L MES 10 g/L Sucrose 3% Phytoagar pH 5.7	4.4 g/L MS 0.5 g/L MES 30 g/L Sucrose 1.5% Phytoagar pH 5.7

Table 2.4 Antibiotics for plant selection

Antibiotics	Stock	Final concentration
PPT	12 mg/mL in ddH_2O	12 µg/mL
Hygromycin	30mg/mL in ddH_2O	15 µg/mL

Bioluminescence analysis

50 mM D-luciferin stock

1 g Firefly D-Luciferin
71.3 mL 1M Triphosphate buffer (Na_2HPO_4 / NaH_2PO_4) pH 8.0

5 mM D-luciferin working solution

1.5 mL 50 mM D-luciferin stock
13.5 mL 0.01% (w/v) Triton-X100

Plant DNA extraction

TE buffer

10 mM Tris-Cl pH 8.0
1 mM EDTA

DNA Extraction Buffer (DEB)

200 mM Tris pH 8.0

240 mM NaCl
25 mM EDTA
1% (w/v) SDS

PCR

Primers (Invitrogen)

dNTP Set, 100 mM Solutions (Fermentas, # R0182)

Taq-DNA polymerase (Genaxxon Bioscience : PeqLab, #01-1000)

Pfu II Ultra® II Fusion HS DNA polymerase (Stratagene, # 600670)

QIAprep® Spin Miniprep kit (Qiagen, #27104)

10 mg/mL Ethidium bromide

6X DNA loading buffer (Fermentas, # R1151)

2X TBE Electrophoresis buffer

67.23 g/L Tris-Cl
34.31 g/L Boric acid
37.22 g/L EDTA pH 8.0

RNA extraction

RNeasy® Plant Mini Kit (Qiagen, #74904)

DNase I recombinant, RNase free (Roche, #04716728001)

Protector RNase Inhibitor (Roche, #03335402001)

qRT-PCR

OligodT primer (Invitrogen)

Superscript® II reverse transcriptase (Invitrogen, #18064-014)

iQ™ SYBR® Green supermix (Bio-rad, #170-8882)

Table 2.5 Primers for qRT-PCR

CCA1	F	TCTGTGTCTGACGAGGGTCGAATT
	R	ACTTTGCGGCAATACCTCTCTGG
LHY	F	CAACAGCAACAACAATGCAACTAC
	R	AGAGAGCCTGAAACGCTATACGA
PRR7	F	TGAAAGTTGGAAAAGGACCA
	R	GTTCCACGTGCATTAGCTCT
PRR9	F	GCACAGAGAAACCAAAGGAA
	R	CTTTCACTCGAGGACGTTGT

Genotyping

GoTaq DNA Polymerase (Promega, #M830B)

Eva green (Biotium, #31000)

Table 2.6 Primers for genotyping Hsp90.2 mutations

Mutant lines	Primers		Changes in amino acid	Mutation sites*
hsp90.2-1	F	TGT TGG CTA ATT CGT GCT TC	G95E	G/A at 284bp
	R	TCC ATG AAT TCC TTG GTT CC		
hsp90.2-4	F	TGT TGG CTA ATT CGT GCT TCT	S100F	C/T at 299bp
	R	CCA GTG CTT CCA TGA ATT CCT		
hsp90.2-6	F	TTG TTT GCT TAC GAT TGT GAT TC	A42T	G/A at 124bp
	R	ACC ATC GAG CTT GCT CTT GT		
hsp90.2-7	F	GCT GAA ACC TTT GCT TTC CA	A11T	G/A at 31bp
	R	CTG ATG AGT TCA CGG AGG AAG		
hsp90.2-8	F	AGC CCA ACA ACA TCA AGC TC	R337C	C/T at 1009bp
	R	TCC GAG GTA CTC AGG GAT GA		

* cDNA information of Hsp90.2 (AT5G56030.1) from TAIR

Gateway cloning

GATEWAY® BP Clonase II enzyme mix (Invitrogen, 11789-020)

GATEWAY® LR Clonase II enzyme mix (Invitrogen, 11791-020)

Table 2.7 Plasmid used for molecular cloning

Plasmid	antibiotic
pDONR201	Kanamycin
pDEST22	Gentamicin
pDEST32	Carbenicillin
pJIC8	Carbenicillin
N-TAP	Spectinomycin
pGEX-6p1	Carbenicillin
pET28b	Carbenicillin
35s::GW::cherry	Carbenicillin
35s::GW::GFP	Carbenicillin

Table 2.8 Primers for cloning cDNAs into pDONR 201/207 (Invitrogen)

Hsp90.2	F	GGG GAC AAG TTT GTA CAA AAA AGC AGG CTT CAT GGC GGA CGC TGA AAC CTT
	R	GGG GAC CAC TTT GTA CAA GAA AGC TGG GTC TTA GTC GAC TTC CTC CAT CT
	R	GGG GAC CAC TTT GTA CAA GAA AGC TGG GTC GTC GAC TTC CTC CAT CTT GC (no stop codon)
CCA1	F	GGG GAC AAG TTT GTA CAA AAA AGC AGG CTT AAT GGA GAC AAA TTC GTC TGG
	R	GGG GAC CAC TTT GTA CAA GAA AGC TGG GTA TGT GGA AGC TTG AGT TTC CT
LHY	F	GGG GAC AAG TTT GTA CAA AAA AGC AGG CTT AAT GGA TAC TAA TAC ATC TGG
	R	GGG GAC CAC TTT GTA CAA GAA AGC TGG GTA TGT AGA AGC TTC TCC TTC CA
PRR7	R	GGG GAC CAC TTT GTA CAA GAA AGC TGG GTC TTA GCT ATC CTC AAT GTT TT (no stop codon)
	F	GGG GAC AAG TTT GTA CAA AAA AGC AGG CTT CAT GAA TGC TAA TGA GGA GGG
	R	GGG GAC CAC TTT GTA CAA GAA AGC TGG GTC GCT ATC CTC AAT GTT TTT TA
PRR9	F	GGG GAC AAG TTT GTA CAA AAA AGC AGG CTT CAT GGG GGA GAT TGT GGT TTT
	R	GGG GAC CAC TTT GTA CAA GAA AGC TGG GTC TCA TGA TTT TGT AGA CGC GT
	R	GGG GAC CAC TTT GTA CAA GAA AGC TGG GTC TGA TTT TGT AGA CGC GTC TG (no stop codon)
ELF3	F	GGG GAC AAG TTT GTA CAA AAA AGC AGG CTT CAT GAA GAG AGG GAA AGA TGA
	R	GGG GAC CAC TTT GTA CAA GAA AGC TGG GTC TTA AGG CTT AGA GGA GTC AT
	R	GGG GAC CAC TTT GTA CAA GAA AGC TGG GTC AGG CTT AGA GGA GTC ATA GC (no stop codon)

Growth media for bacteria

Luria Bertani (LB)

10 g/L Bacto-tryptone
5 g/L Yeast extract
5 g/L NaCl
1% Agar
pH 7.5

YEBS

5 g/L Beef extract
5 g/L Peptone
5 g/L Sucrose

1 g/L Yeast extract
0.5 g/L $MgSO_4$
1% agar
pH 7.0

Table 2.9 Antibiotics for bacteria selection

Antibiotics	Stock	Final concentration
Gentamicin	100 mg/mL in ddH_2O	10 μg /mL
Carbemicilin	100 mg/mL in ddH_2O	100 μg /mL (E. coli)
		50 μg/mL (Agrobacterium)
Kanamycin	100 mg in ddH_2O	50 μg /mL
Chloramphenicol	10 mg/mL in ethanol	30 μg /mL
Rifampicin	25 mg/mL in methanol	25 μg /mL
Spectinomycin	30 mg/mL in ddH_2O	30 μg /mL
Streptomycin	30 mg/mL in ddH_2O	30 μg /mL

Extraction and purification of E.coli expressed proteins

Table 2.10 Buffers for protein extraction and purification

Lysis buffer	Wash buffer	Elution buffer
50mM NaH_2PO4	50mM NaH_2PO4	50mM NaH_2PO4
300mM NaCl	300mM NaCl	300mM NaCl
10mM imidazole	20mM imidazole	250mM imidazole
pH 8.0	pH 8.0	pH 8.0

1X PBS

8g NaCl
1.54g $Na_2HPO_4 \cdot 12H_2O$
0.29g KH_2PO_4

1% Triton-X100/PBS

1% Triton-X100
1X PBS

5mM Glutathion solution

15.4mg Glutathion powder
5ml 50mM Tris-Cl pH 8.0

Dialysis buffer

10mM Tris-Cl pH 8.0
30% Glycerol

In vitro binding buffer

Binding buffer

50mM Tris-Cl pH7.5
1mM EDTA
150mM NaCl
0.1% Triton X-100
10% Glycerol
1X BSA

Tobacco Agro-infiltration

Infiltration solution

1 mM $MgCl_2$
1 mM MES
ddH_2O

MES

MS (4.4G/L)
10% Sucrose
2.6mM MES
pH 5.8 (adjust pH with KOH)

Co-immuneprecipitation buffer

IP buffer

50mM Tris-Cl pH 8.0
150mM NaCl
1mM EDTA
10% Glycerol
1% Triton X-100
½ tablet/10mL cOmplete® EDTA-free tablets
50mM MG132

Washing buffer

50mM Tris-Cl pH 8.0
140mM NaCl
1mM EDTA
0.1% Triton X-100

Protein extraction

Denaturation buffer

100mM NaH2PO4
10mM Tris-Cl (pH8)
8M Urea

SDS-PAGE

SDS-PAGE gel

Table 2.11 Separation gel for 1.5mm case

Gel concentration	ddH2O (mL)	Seperation buffer (mL)	Acrylamide (mL)	APS (μL)	TEMED (μL)
8%	4	2	2	50	5
15%	2	2	4	50	5

Table 2.12 Stacking gel for 1.5mm case

ddH2O (ml)	Stacking buffer (ml)	Acrylamide (ml)	APS (μL)	TEMED (μL)
2.25	0.94	0.5	22.5	7.5

Speration buffer

1.5M Tris
0.4% SDS
pH 8.8

Stacking buffer

0.5M Tris
0.4% SDS
pH 6.8

5X SDS gel running buffer (1L)

15.17g Tris
72g glycine
5g SDS

5X SDS sample buffer

0.225M/Tris-Cl pH 6.8
50% glycerol
5% SDS
0.25% bromophenol
0.25M DTT

Comassie Blue staining solution

0.25g Comassie Blue
100mL of destaining solution

Destaining solution

500mL methanol
400mL ddH_2O
100mL acetic acid

Western blot

Transfer buffer

25mM Tris
192mM glycine
10% methanol

10X PBS-T

80g NaCl
15.395g $Na_2HPO_4 \cdot 12H_2O$
2.905g KH_2PO_4
5mL Tween

2.2 Methods

2.2.1 Seed sterilization

Seeds were placed in clean 1.5mL eppendorf tubes. Seeds were rinsed with 800µl of 100% ethanol for 2 minutes. Afterwards, ethanol was removed and seeds were rinsed with 800µl of bleach solution for 2 minutes. The bleach solution was removed and seeds were washed with 900µl of sterile water. Finally the seeds were suspended in sterile 0.01% agar water. Seeds were plated on the appropriate MS agar plate with specific antibiotics listed in Table 2.5 (if required). The plated seeds were kept at 4°C for 2-3 days in the dark, and then transferred to the growth cabinet.

2.2.2 Bioluminescence

Seedlings were entrained for 7 days in the growth carbinet. On day 7, seedlings were transferred to black 96-well Microplates (OPTIPLATE TM-96F, PerkinElmer) containing 200µl of MS3 agar in each well. After seedlings were successfully transferred, 15µl of 5mM Luciferin was added to each well and plates were sealed with transparent film. Finally, each well was perforated using a needle. An additional day of entrainment in the growth cabinet was applied before plates were transferred to the TOPCOUNT® (PerkinElmer). The tri-chromatic LED panels were attached to the stackers which loads the plates.The LED panels can output red light, blue light and far red light individually or combination of these three light source. The room temperature was normally set at 22°C.

The luminescence signals were collected by the TOPCOUNT®. Data was visualized and analyzed by using TOPTEMP II macro and Biological Rhythms Analysis Software System 2.1.2 (BRASS) macro for EXCEL (Southern and Millar, 2005). For period analysis, period values weighted by relative amplitude error (RAE) were considered. RAE was the value of the amplitude error estimate divided by the value of the most probable amplitude estimate. This means that RAE is a measure of how well the actual data fit to the cosine curve generated by the least-squares method. Theoretically, RAE can range from 0 to 1. When RAE=0, the rhythm curve perfectly fits the cosine curve. When RAE=1, the curve is entirely arrhythmic.

For phase response curve (PRC) assay, plants were grown for 7 days under LD condition (12 hours in light and 12 hours in darkness) and then transferred on to TOPCOUNT® with red and blue light on for one full day before 3 hours 27°C heat pulses were applied every 3 hours to each 96-well plate one after another. The time of the first peak after heat pulse was picked and the time difference between pulsed and non-pulsed populations was calculated (Covington et al., 2001).

2.2.3 Plant DNA extraction

In order to extract DNA from Arabidopsis, firstly, the plant tissue was held in 1.5mL eppendorf tube with 100µl DNA extraction buffer (DEB) and ground at room temperature (RT). Then, an additional 400µl of DEB and 100µl chloroform was added, followed by a 5-minute vortex. The tubes were centrifuged for 10 minutes at the maximum speed (14,000rpm). A total of 350µl of supernatant was transferred to a new tube and mixed with an equal volume of isopropanol. Another 10-minute centrifuge and the supernatant was discarded. The pellet was rinsed by 500µl 70% (v/v) ethanol. Ethanol was then removed after another 5-minute centrifuge (14,000rpm). Finally, the pellet was air-dried and resuspended in 100µl 1X TE buffer. Additionally, the concentration of DNA was measured by NanoDrop 1000 spectrophotometer (Peqlab).

2.2.4 Gene cloning

For the PCR amplification of the *Hsp90.2* and the clock genes, the PCR mixture was prepared as follow:

10x Pfu Ultra II buffer	5.0µl
dNTP	5.0µl
DNA	1.0µl
Primer mix	2.0µl
Pfu Ultral II DNA polymerase	1.0µl
H_2O	36.0µl
Total	50.0µl

Primers used for PCR are listed in Table 2.9.

2.2.5 Genotyping

To genotype Arabidopsis, especially to test for single mutation sites, genomic DNA was extracted from individual seedlings. The following mixtures were prepared before for melt curve genotyping in the LightCycler 480 II (Roche):

2x Eva buffer (1µL)	
Water	0.69µL
EBB	0.1µL
dNTPs	0.04µL
GoTaq	0.02µL
Eva green	0.15µL
Total	1 µL

PCR reaction mixture (for 1 reaction)	
Water	3.6µL
2x Eva buffer	5µL
Primer (f)	0.2µL
Primer (r)	0.2µL
DNA	1µL
Total	10µL

Program setting and data analysis followed the Manual of LightCycler 480 II (Roche).

2.2.6 Cloning with Gateway

All Gateway® empty vectors were propagated in *Escherichia coli (E. coli) DB3.1* cells. *E. coli DH5α* cells were used to propagate transformed vectors. BP reaction was performed to recombine PCR products into pDONR201. The BP reaction was set up as follow:

Target DNA	0.5µl (≈100fmol)
pDONR201	0.5µl (≈100fmol)
TE buffer	3µl
BP Clonase Enzyme mix	1µl
Total	5µl

The reaction was left at 25°C for at least 6 hours. After that, 1µl of this reaction mix was used to transform *E. coli DH5α* cells.

LR reaction was performed to transfer targert genes from entry vectors to destination vectors. LR reaction was set up as follow:

pDONR201	0.5µl
Destination vector	0.5µl
TE buffer	3µl
LR Clonase Enzyme mix	1µl
Total	5µl

The reaction was left at 25°C for at least 6 hours. Then, 1µl of LR reaction was used to transform *E. coli DH5α* cells.

2.2.7 E.coli transformation

For *E. coli* transformation, an aliquot (50µl) of chemical-competent *E. coli* cells was thawed on ice and 1µl of plasmid was added to the cells. After being left on ice for 30 minutes, the cells were heated at 42°C for 1-2 minutes. Then the cells were immediately moved onto ice and cooled for 2 minutes. After that, 500µl of LB media was added to the cells, and they were incubated at 37°C for 1 hour, with gentle shaking. After incubation, 100µl of the cell suspension was plated on an appropriate selective LB agar plate. Plates were sealed with parafilm and incubated overnight at a 37°C.

2.2.8 Isolation of Plasmid DNA

A single colony growing on the selective plate was picked and inoculated in 10mL of selective LB media. The cells were cultured at 37°C for approximately 16 hours. Then the cells were collected by centrifuging at 4000rpm for 10 minutes. Plasmid was extracted by using the Qiaprep® Spin Miniprep Kit (Qiagen). Finally, DNA concentration was measured by NanoDrop 1000 spectrophotometer (Peqlab).

2.2.10 Isolation and purification of proteins

To express proteins in *E. Coli* BL21 (DE3) or *E. Coli* Rosetta, 10mL cells were pre-cultured in selective LB media overnight. From 10mL culture, 2mL of cell culture was added to 300mL fresh selective LB medium. The new culture was subsequently incubated at 37°C until its OD600 reached 0.8-1.0. IPTG was added to induce protein expression (1mmol IPTG for pET28b plasmid). Then, the cell culture was incubated at

18°C overnight. On the next day, cells were collected by centrifuging at 4000rpm for 10 minutes. To isolate the protein, 10mL lysis buffer together with 1 piece of proteinase inhibitor was added to the cells and these cells were broken by sonification. After that, particulate material was pelleted by centrifugation at 13,000rpm for 30 minutes. Meanwhile, 1mL Ni-NTA Agarose was rinsed by 10mL lysis buffer for 3 times in 15mL falcon tube. After centrifuging, the clarified supernatant was loaded onto the Ni-NTA Agarose beads. For maximal binding of the His- tagged protein, the tube was rotated for 2 hours at 4°C. The fully bound Ni-NTA Agarose beads were spun down at 500rpm for 2 minutes and the supernatant was removed. The Ni-NTA Agarose beads were twice rinsed by 10mL wash buffer and resuspended in 10mL wash buffer before loaded onto an empty column. The flow through wash buffer was discarded. In the end, the His-tagged protein was eluted by 10mL elution buffer.

To isolate and purify GST-tagged proteins (encoded by pGEX6p-1 plasmid), the *E.coli* culture was harvested, and the cells were washed with 1X PBS and centrifuged. The pellet was resuspended in 10mL of 1X PBS. Afterwards, 100µl of lysozyme (100 mg/mL) was added, followed by a 15-minute incubation on ice. One tablet of proteinase inhibitor was added and the cells were sonicated. After sonication, 1% of Triton X-100/PBS was added. This mixture was centrifuged at 10000rpm at 4°C for 20 minutes after rocked at 4°C for 30 minutes. During the centrifuge, 100µl of glutathione sepharose 4B resin was prepared and equilibrated with 1X PBS three times. After centrifuge, the clarified supernatant was rocked with pre-equilibrated resin at 4°C for 2 hours. The resin was collected by centrifuging at 1500rpm for 5 minutes and washed by 1X PBS. In the end, the GST-tagged protein was eluted with 5mM, 10mM, or 20mM glutathione solutions.

2.2.11 in vitro protein binding assay

To identify if proteins interacted with each other *in vitro*, 2µg His-tagged protein were mixed with 2µg GST-tagged protein, binding buffer and Ni-NTA agarose, and then was incubated at 4°C for 2 hours. The Ni-NTA agarose was spun down at 8000rpm at 4°C and washed with 400µl of binding buffer. This was repeated for 4 times. In the end, 50µl 1X SDS sample buffer was added and boiled at 95°C for 5 minutes. This sample was ready for SDS-PAGE.

2.2.12 Western blot

To transfer proteins onto Immobilon-P membrane (Millipore), the membrane was activated by rinsing with 100% methanol. Protein transferring was done with Mini-PROTEAN® Tetra System (Bio-rad). The cassette including protein gel, membrane and paper was assembled and inserted into the tank filled with transfer buffer. For transferring, constant voltage was set at 100V for 1mm gel.

After transferring, the membrane was immediately incubated in 5% milk/PBS-T for 30 minutes. After briefly washed with 1X PBS-T, the membrane was incubated with primary antibody in 5mL 1X PBS-T at 4°C overnight. The membrane was washed with 1X PBS-T for 4 times before incubated with secondary antibody in 1X PBS-T for 2 hours. In the end, after washed for 4 times, to visualize the protein, the membrane was incubated with solution A and solution B (GE Healthcare) in 1X PBS-T for 5 minutes before developments in the dark room.

2.2.13 Agrobacterium transformation

Agrobacterium tumefaciens (*Agrobacterium*) strain ABI (Schomburg et al., 2001) was used. An aliquot (50µl) of electrocompetent cells was thawed on ice. Then, 1µl of plasmid and 80µl of sterile ddH_2O were added to the cells. The diluted cells were transferred to an electroporation cuvette for electroporation. After electroporation, cells were immediately mixed with 900µl of LB media and transferred to 1.5mL eppendorf tube. After incubated for 2 hours at 28°C, 100µl of the cell culture was plated on selective YEBS agar plate. Plates were sealed with parafilm and incubated at 28°C for 2 days to allow for colony growth (Weigel and Jurgens, 2002).

2.2.14 Tobacco infiltration

Agrobacterium cells were cultured in 100mL selective YEBS media for 2-3 days at 28°C at 250rpm. Before infiltration, the cell cultures were centrifuged at 4000rpm for 10 minutes, and the supernatant was discarded. Pellets were resuspended in infiltration buffer. Cell density was determined by measuring OD600. The resuspended cells were diluted with infiltration buffer to OD 1.0. Then, 1µl of 1M acetosyringone was added and the cultures were left in the darkness at room temperature for 3 hours. Appropriate bacterial strains were mixed with the

Agrobacterium strain P19 harboring the expression vector (Voinnet et al., 2003). Bacterial mixtures were infiltrated into *N. bentamiana* leaves with a 1mL syringe. Plants were watered several hours before the infiltration. After infiltration, plants were kept in the greenhouse for 3 days before microscope observation or sample collection.

2.2.15 Co-immunoprecipitation

The deep-frozen infiltrated tobacco leave tissue was ground with TissueLyser (Retsch MM301) for 1 minute at frequency of 1/30s. Then, 1mL of IP buffer was added before centrifuging at 14,000rpm for 15 minutes at 4°C. Afterwards, the supernatant were loaded onto pre-equilibrated GFP trap beads and incubated at 4°C for 2.5 hours on an orbital shaker. After incubation, the GFP trap beads were washed with 1mL washing buffer. This was repeated for 4 times. In the end, the buffer was removed and 50µl of 2X SDS sample buffer was added, followed by a boiling at 95 °C for 5 minutes.

2.2.16 RNA extraction

Arabidopsis seedlings were grown for 7 days. Around 100 mg seedlings was harvested and transferred to a 1.5mL eppendorf tube together with two metal beads. Immediately the tube was frozen in liquid nitrogen. To grind the harvested samples, tubes containing samples were loaded onto TissueLyser (Retsch MM301). The grinding took 30 seconds for Arabidopsis tissue. During the grinding process, tissue sample was kept frozen. RNeasy® Plant Mini Kit was used to extract RNA. In the end, the RNA was resuspended in 80µl RNase-free water.

Before performing DNA digestion, resuspended RNA was centrifuged at 14,000rpm at 4°C for 30 minutes. Then, 70µl of the supernatant was transferred to a fresh tube. To do this, 2µl DNase, 1µl RNase inhibitor and 8µl DNase recombinant buffer were added. This was incubated at 37°C for 2 hours.

Subsequently, RNA was precipitated by adding 8µl 3M NaAc (pH 5.2) and 160µl 100% ethanol. The precipitation lasted overnight at -20°C. RNA was collected by centrifuging at 14000rpm at 4°C for 1 hour. The supernatant was removed and the pellet was washed three times with 100% ethanol. In the end, the pellet was resuspended in 32µl RNase-free water. From this 32µl RNA, 1µl was used to

measure the RNA concentration by using NanoDrop 1000 (Peqlab) and 1µl was used as template to check for genomic DNA contamination.

2.2.17 Reverse transcription

cDNA was generated by RNA reverse transcription. Before reverse transcription, RNA concentration was measured and 3µg RNA was taken for reverse transcription. Reverse transcription was performed, according to cDNA synthesis protocol for Superscript® II RT (Invitrogen).

2.2.18 qRT-PCR

Enrichment of DNA sequences was measured by qRT-PCR. Primers were designed using Primer3Plus (Untergasser et al., 2007) to obtain amplicon sizes that ranged from 150-200bp (Table 2.5). qRT-PCR was performed with iQ™ SYBR® Green supermix (Bio-rad) on the LightCycler 480 II (Roche).

2.2.19 Confocal imaging

For all microscopy experiments, a Zeiss LSM 780 confocal laser scanning microscope and Zeiss ZEN 2011 Software was used. *N. benthamiana* leaf excisions and *A. thaliana* seedlings were submerged in water. The spectral settings were as follows: for GFP, excitation 488 nm and emission 505-580nm; for mCherry RFP, excitation 587nm and emission spectra 605-700nm.

Chapter 3 Hsp90 contributes to the clock

Some of the results in this chapter represent collaborative work:

Koumis philippou performed Topcount assay in Figure 3.1

Amanda Davis performed Topcount assay in Figure 3.2

Amanda Davis analyzed the data of phase response curve in Figure 3.4.

3.1 Introduction

Recent studies showed that Hsp90 is involved in the regulation of the clock. Inhibition of cytoplasmic Hsp90 by Hsp90-specific inhibitor GDA and RNAi-mediated depletion results in a long period phenotype (Kim et al., 2011). Hsp90 is a heat-induced protein chaperon. As such, I tested if Hsp90 affects the clock phenotype under temperature conditions.

At the molecular level, the clock component ZTL was proposed to be the client of Hsp90. GI was demonstrated to be linked with Hsp90 in the posttranslational regulation of ZTL (Kim et al., 2011). However, my data showed that GDA lengthened the period of *ztl* mutant, which indicated that ZTL may be the only target of Hsp90. Thus, I tested other clock genes to reveal the potential targets of Hsp90.

In this chapter, the phase response assay revealed that Hsp90.2 is involved in the clock regulation pathway before dawn. CCA1, LHY, PRR7, PRR9, GI, and ELF3 are all activated and highly expressed within this time window. As previously shown, ELF3, PRR7, and PRR9 are key components in temperature entrainment (Salome and McClung, 2005; Salome et al., 2010) (McWatters et al., 2000; Thines and Harmon, 2010). The morning clock loop (CCA1, LHY, PRR7, and PRR9) and GI were identified to be involved in the temperature-compensation mechanism (Salome et al., 2010) (Gould et al., 2006). Therefore, I examined these potential targets by applying GDA to the clock mutants of Arabidopsis.

Core clock components CCA1 and LHY are highly likely to be targets of Hsp90.2, as the clock period of their mutants were not influenced by GDA. However, I confirmed that CCA1 and LHY are not the direct targets of Hsp90.2. As PRR7 and PRR9 are transcription repressors of *CCA1* and *LHY* (Nakamichi *et al*., 2010; Nakamichi *et al*., 2005), therefore, I tried to identify if CCA1 and LHY are indirect targets of Hsp90.2 through PRR7 and PRR9.

Finally, PRR7 and PRR9 were proved to be involved in the Hsp90.2 regulation pathway in this chapter, but they were not the direct targeted by Hsp90.2. However, ELF3 was demonstrated to repress transcription of PRR9 (Eva, 2012). Therefore, I tested if ELF3 has a direct interaction with Hsp90.2.

3.2 Results

3.2.1 Hsp90 is involved in the clock regulation pathway

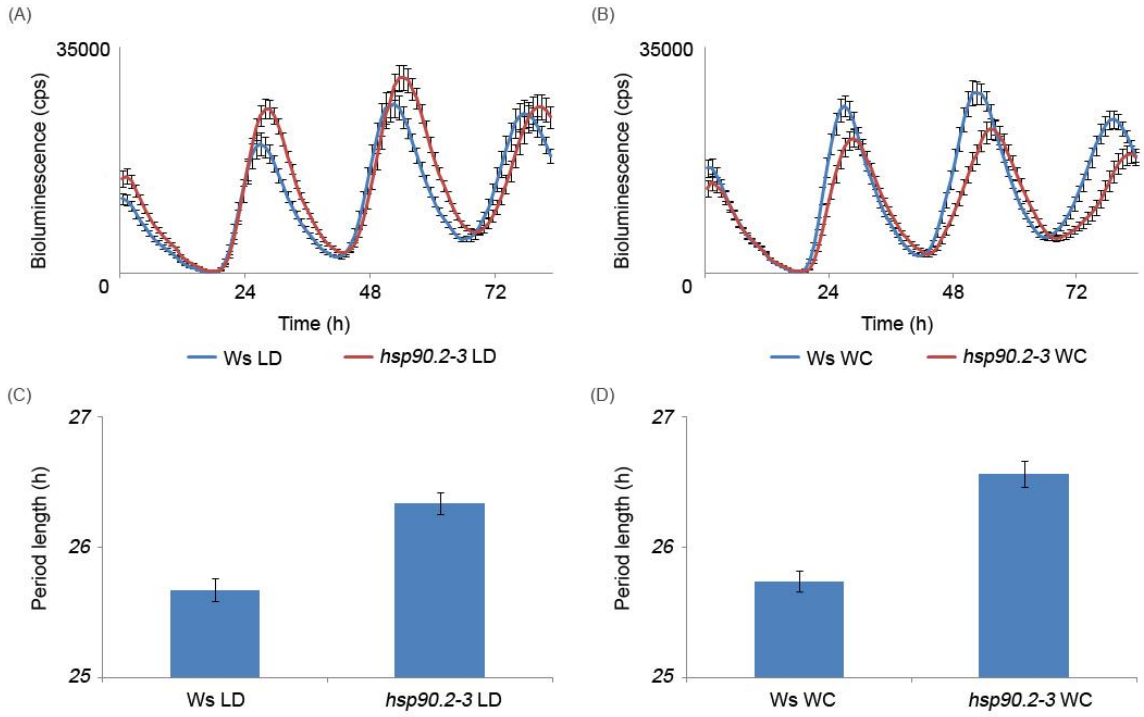

Figure 3.1 The hsp90.2-3 mutation resulted in a more pronounced long-period phenotype under both LD and WC conditions.

(A) Bioluminescence of *CCR2:LUC* under LD condition. (B) Bioluminescence of *CCR2:LUC* under WC condition. (C) Period length of *CCR2:LUC* under LD condition. Ws LD, 25.68±0.09h; *hsp90.2-3*, 26.34±0.08h. (D) Period length of *CCR2:LUC* under WC condition. Ws LD, 25.74±0.08h; *hsp90.2-3*, 26.56±0.10h. Error bars indicate SEM, n=48. LD = light-dark. WC = warm-cool.

To test if Hsp90 contributes to oscillator behavior, the *hsp90.2* known alleles were analyzed (Hubert et al., 2009). The *hsp90.2-3* was one of these mutants and was first used to test Hsp90 function on clock activity. After (light-dark) LD entrainment condition, the *hsp90.2-3* mutant had a period of 26.34h, slightly longer than Ws wild type, whose period length was 25.68h (Figure 3.1A, C). More pronounced than LD condition, under WC condition, the *hsp90.2-3* mutant achieved a 26.56h daily cycle, longer than that 25.74h of Ws wild type (Figure 3.1B, D). Therefore, the period phenotype difference under both conditions suggested that Hsp90 could influence plant circadian clock.

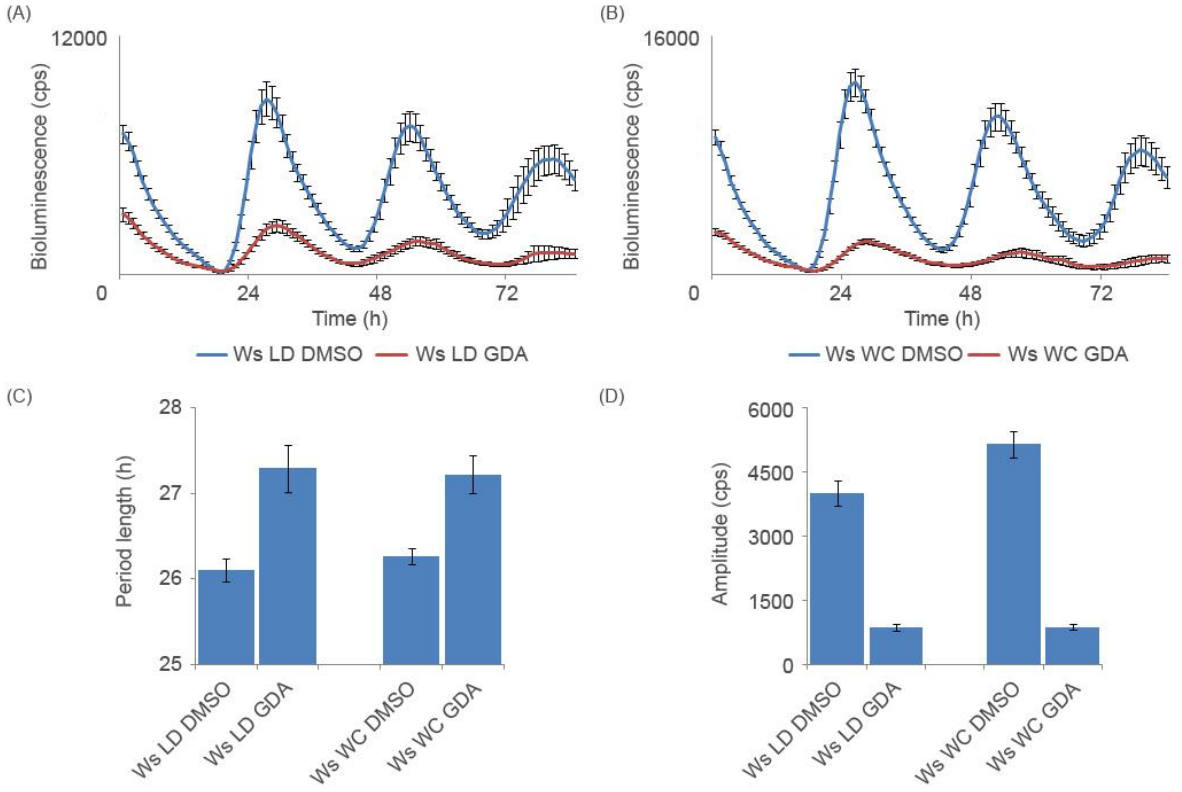

Figure 3.2 GDA lengthened circadian period and reduced the circadian robustness under both LD and WC conditions.

(A) Bioluminescence of *CCR2:LUC* under LD condition. (B) Bioluminescence of *CCR2:LUC* under WC condition. (C) Period length of *CCR2:LUC* under LD and WC conditions. Ws LD DMSO, 26.10±0.13h; Ws LD GDA, 27.30±0.28h; Ws WC DMSO, 26.27±0.09h; Ws WC GDA, 27.23±0.23h. (D)Robustness of *CCR2:LUC* under LD and WC conditions. Ws LD DMSO, 4013.97±288.48cps; Ws LD GDA, 870.58±86.31cps; Ws WC DMSO, 5152.67±314.95cps; Ws WC GDA, 878.26±64.87cps. Error bars indicate SEM, n=48. LD = light-dark. WC = warm-cool.

Hsp90 has several isoforms in Arabidopsis (L.H. Pearl, 2006). To mimic the total *hsp90* loss-of-function mutation, Ws wild-type seedlings were treated with 2μM GDA. The optimal concentration (2μM) of GDA was determined by dose-response assay. After either photic or thermal entrainment, GDA triggered a longer period, which was similar to *hsp90.2-3* mutation (Figure 3.2A, B, C). Additionally, GDA dampened the bioluminescence signals and reduced robustness of circadian clock (Figure 3.2A, B, D). These pharmacological data by GDA phenocopied the *hsp90.2-3* effect and provided confirmation that Hsp90 is involved in clock regulation.

To ensure that the phenotype caused by *hsp90* loss-of-function did not specifically exist in Ws background with *CCR2:LUC* promoter. Bioluminescence assays were repeated in Col background with *TOC1:LUC* promoter. The results are consistant with those in Ws background (Figure 3.3). These replicates in Col background showed that Hsp90 broadly existed in Arabidopsis clock regulation system.

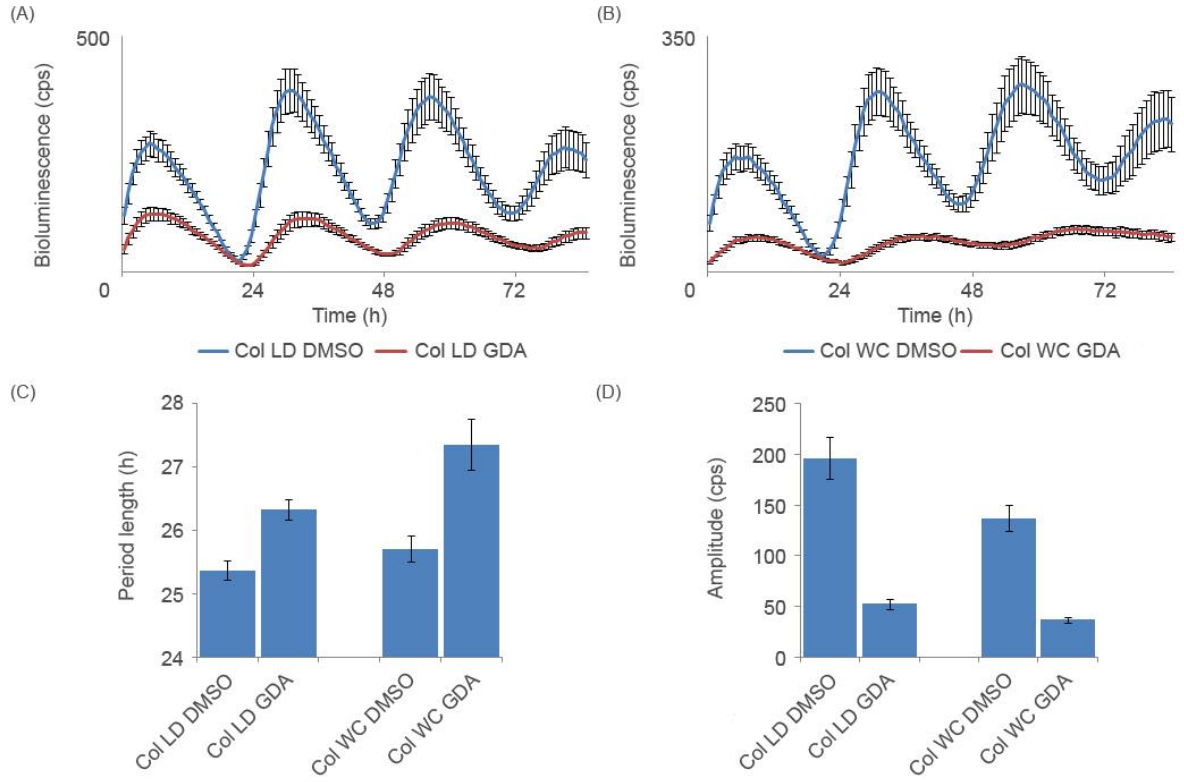

Figure 3.3 GDA lengthens circadian period and reduced the circadian robustness in Col background under both LD and WC conditions.

(A) Bioluminescence of *TOC1:LUC* under LD condition. (B) Bioluminescence of *TOC1:LUC* under WC condition. (C) Period length of *TOC1:LUC* under LD and WC conditions. Col LD DMSO, 25.37±0.15h; Col LD GDA, 26.34±0.16h; Col WC DMSO, 25.71±0.21h; Col WC GDA, 27.36±0.40h. (D)Robustness of *TOC1:LUC* under LD and WC conditions. Col LD DMSO, 196.64±20.19cps; Col LD GDA, 52.91±5.03cps; Col WC DMSO, 137.24±13.07cps; Col WC GDA, 37.13±2.80cps. Error bars indicate SEM, n=48. LD = light-dark. WC = warm-cool.

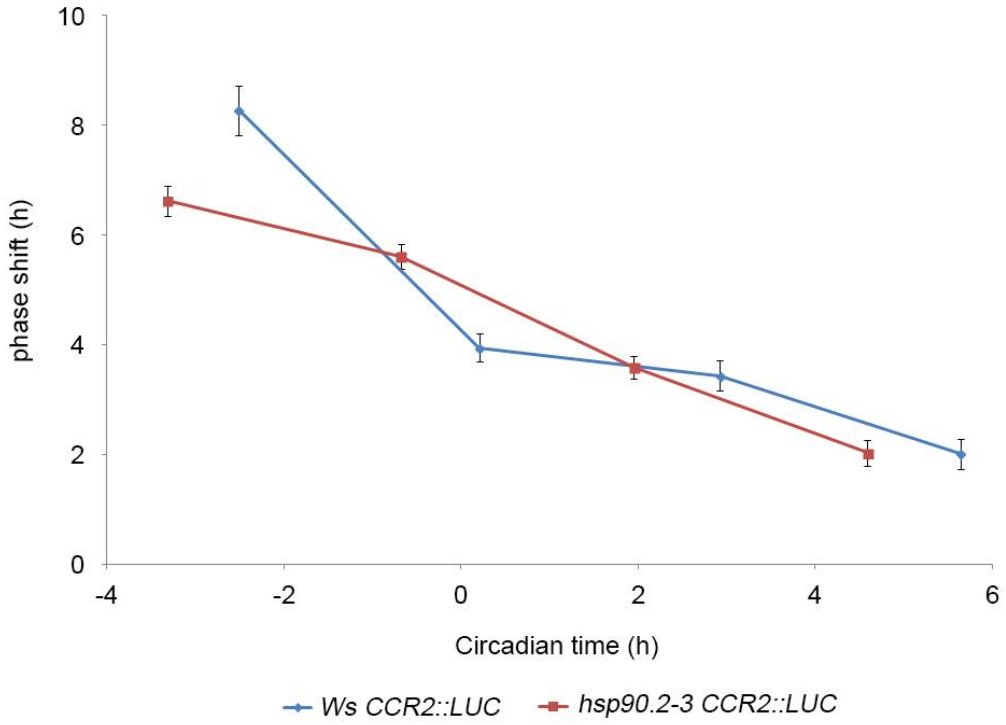

Figure 3.4 Ws wild type and hsp90.2-3 mutant responded to heat shock differently at late night and early morning.

The phases were shifted due to the heat shock (27°C). The X axis shows different circadian time points, at which the plant phases data were collected. The time point "0" is the time when light is on. The Y axis is the phase differences between the heat-shocked plants and the negative control, the non-heat-shocked plants. Error bars indicate SEM, n=48.

I performed the phase response assay to identify how Hsp90 contributes to the temperature regulation on the clock at different times. The responses to heat shock were different between *hsp90.2-3* and Ws wild type before dawn. At ZT(-3), the Ws wild type had an 8h phase shift whereas the *hsp90.2-3* mutant had a 6h phase shift, 2h lower than the Ws wild type. It was similar at ZT0 when the light was just on. There was a 2h difference between *hsp90.2-3* and the wild type. During the morning time, at ZT3 and ZT6, there was almost no significant difference between *hsp90.2-3* and Ws wild type (Figure 3.4). In conclusion, the pre-dawn phase shifts indicate that Hsp90 assists circadian clock to keep stable before dawn.

3.2.2 Hsp90 affects circadian clock through morning clock genes

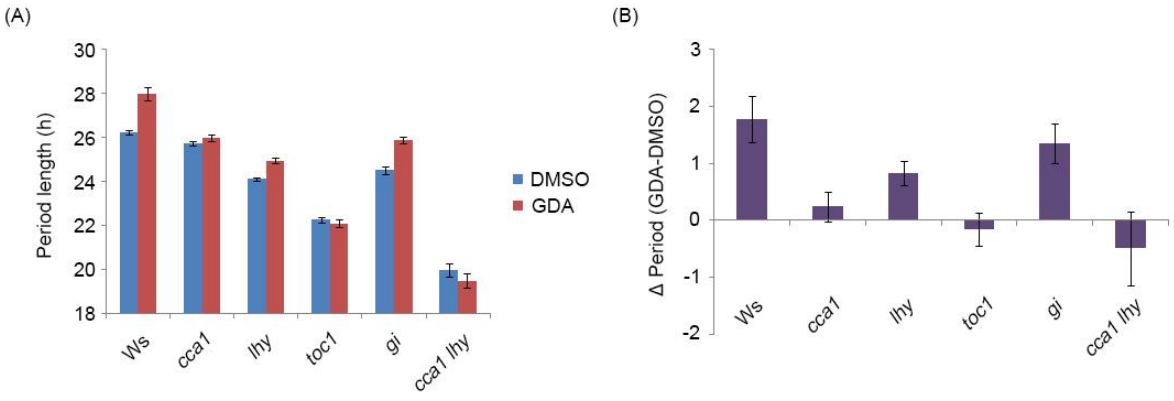

Figure 3.5 Morning-clock-gene mutants were not GDA sensitive.

(A) The blue and red bars represent period length of *CCR2:LUC* under WC condition with DMSO treatment and with GDA treatment, respectively. Ws DMSO, 26.22±0.11h; Ws GDA, 28.00±0.29h; *CCA1* DMSO, 25.73±0.11h; *CCA1* GDA, 25.97±0.15h; *lhy* DMSO, 24.13±0.07h; *lhy* GDA, 24.96±0.13h; *toc1* DMSO, 22.27±0.11h; *toc1* GDA, 22.10±0.18h; *gi* DMSO, 24.51±0.19h; *gi* GDA, 25.87±0.16h; *CCA1 lhy* DMSO, 20.00±0.30h; *CCA1 lhy* GDA, 19.50±0.34h. (B) The purple bars represent the difference of period length between DMSO-treated seedlings and GDA treated seedlings. Error bars indicate SEM, n=48.

I assumed that Hsp90, as a chaperone, affects the clock by regulating known clock components, including CCA1, LHY, TOC1, and GI. As shown in Figure 3.3 and 3.4, by inhibiting Hsp90, GDA phenocopied the Hsp90.2 loss-of-function mutant. Applying GDA to clock mutants could identify if the effect of this Hsp90 inhibition on circadian clock requirs CCA1, LHY, TOC1, or GI. If the effect on circadian clock is dependent on these clock components, their mutants should not show a lengthened period. For the *cca1*, *lhy*, *toc1*, *gi* and *cca1 lhy* mutants, the period were all shorter than Ws wild type (Figure 3.5A). The GDA-treated Ws wild-type seedlings showed a longer period, compared to non-treated seedlings. This GDA effect was also observed in the *gi* mutant. However, in the *cca1* and *toc1* mutants, GDA had almost no effect on period length. In the *lhy* mutant, the effect of GDA was weaker. Moreover, in the *cca1 lhy* double mutant, GDA even shortened the period length (Figure 3.5A, B). To conclude, as period length of the *cca1*, *lhy*, *toc1* mutants were not affected by GDA. Taken together, CCA1, LHY, and TOC1 were identified genetically as potential transcriptional targets of Hsp90.

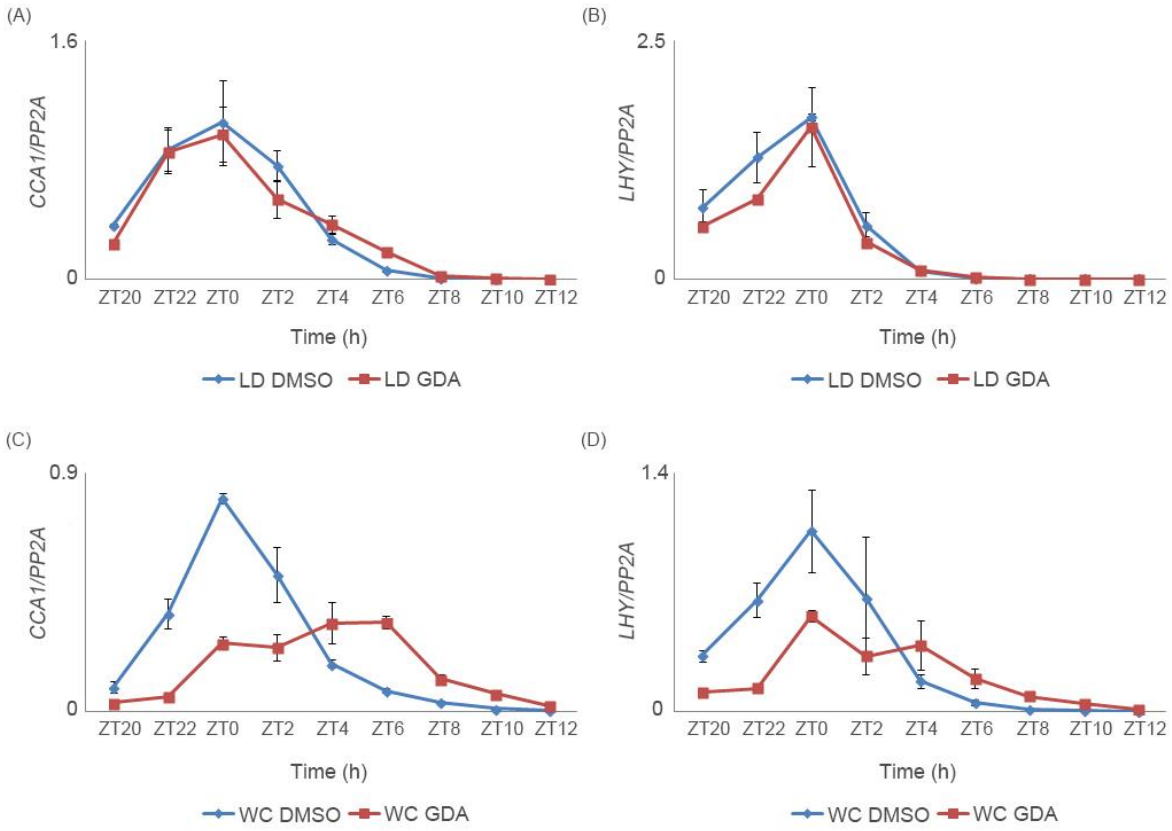

Figure 3.6 Accumulation of CCA1 and LHY were altered by GDA under WC condition.
(A) and (B), accumulation of *CCA1* and *LHY* are not affected by GDA under LD condition. (C) and (D), accumulation of *CCA1* and *LHY* are altered by GDA under WC condition. Samples were collected every 2 hours from ZT20 to ZT12 next morning. Expression values are normalized to *PP2A* and are representative of three biological replicates. Error bars indicate SD.

As shown in the phase response assay, Hsp90 contributed to pre-dawn clock function (Figure 3.2). Furthermore, I identified that morning component *CCA1* and *LHY* were genetically required by Hsp90. Therefore, I first checked gene expression of *CCA1* and *LHY* under both LD and WC conditions, respectively. Under LD condition, accumulation of *CCA1* and *LHY* were not affected by GDA (Figure 3.6A, B). However, under WC condition, GDA-treated seedlings have reduced accumulation of *CCA1* and *LHY* at early morning and increased accumulation *CCA1* and *LHY* after ZT4, compared to the non-treated seedlings. The accumulation curve turned “flatter” with “fatter” tails as the day progressed (Figure 3.6C, D). For *CCA1*, it no longer peaked at ZT0. Instead, accumulation of *CCA1* maintained at a relatively high level from ZT0 to ZT6 (Figure 3.6C). For *LHY* accumulation, GDA resulted in the similar

effect as *CCA1* (Figure 3.6D). In conclusion, although GDA caused a longer period phenotype in Arabidopsis under both LD and WC condition, here the qRT-PCR results indicated that the way Hsp90 regulated the clock might be different. Under WC condition, Hsp90 profoundly regulated the accumulation of *CCA1* and *LHY*.

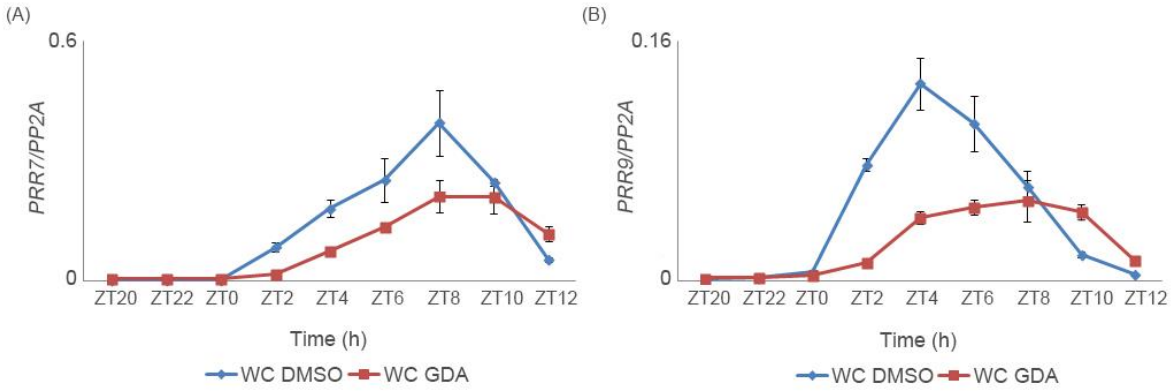

Figure 3.7 Accumulation of PRR7 and PRR9 were altered under WC condition.

(A) and (B) Accumulation of *PRR7* and *PRR9* are altered by GDA under WC condition. Samples were collected every 2 hours from ZT20 to ZT12 next morning. Expression values are normalized to *PP2A* and are representative of three biological replicates. Error bars indicate SD.

Hsp90 potentially regulated the morning clock components *CCA1* and *LHY*. PRR7 and PRR9 were proposed to inhibit transcription of *CCA1* and *LHY* by binding to their promoter regions (Farre EM, 2005). Hsp90 was likely to indirectly regulate transcript accumulation of *CCA1* and *LHY* through PRR7 and PRR9. Therefore, I tested if *PRR7* and *PRR9* were likely targets of Hsp90. Examining transcript accumulation as above, I first checked the wave-form of *PRR7* and *PRR9*. Similar to *CCA1* and *LHY*, accumulation of *PRR7* and *PRR9* were affected by GDA and both were reduced. Particularly, the transcription curve of *PRR9* was shifted and the peak value was reduced by more than half. Therefore, in addition to *CCA1* and *LHY*, transcript abundance of *PRR7* and *PRR9* were also regulated by Hsp90.

3.2.3 Hsp90 regulates transcription of *CCA1* and *LHY* through PRR9

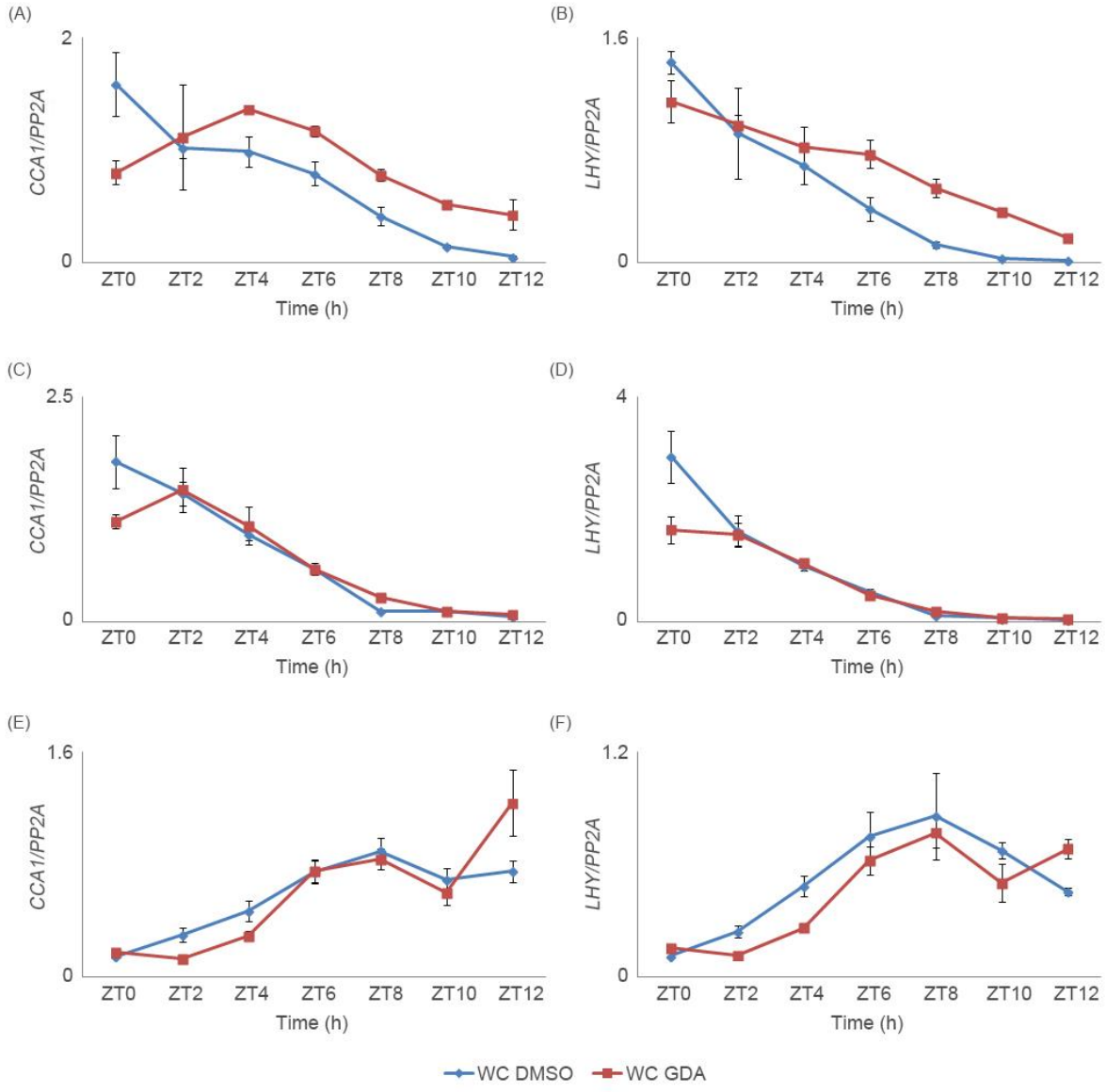

Figure 3.8 Accumulation of CCA1 and LHY are not altered in prr9 mutants in the morning.
(A) and (B) Accumulation of *CCA1* and *LHY* in *prr7* mutant are altered in the morning. (C) and (D) Accumulation of *CCA1* and *LHY* remain unchanged in *prr9* mutant in the morning. (E) and (F) Accumulation of *CCA1* and *LHY* in *prr7 prr9* mutant remain unchanged in the morning. Samples were collected every 2 hours from ZT0 to ZT12 next morning. Expression values were normalized to *PP2A* and are representative of three biological replicates. Error bars indicate SD.

As previously mentioned, it was proposed that gene accumulation of *CCA1* and *LHY* are inhibited by PRR7 and PRR9. Therefore, my hypothesis was that Hsp90 could affect transcription of *CCA1* and *LHY* through PRR7 and PRR9. To genetically

test this, I applied GDA to *prr7*, *prr9*, and *prr7 prr9* mutants and focused on gene transcription in the morning. In GDA-treated *prr7*, transcription levels of *CCA1* and *LHY* exceeded the non-treated ones after ZT4, which was similar to the Col wild type (Figure 3.8A, B). Accumulation of *LHY* diverged more significantly from ZT6 to ZT10 (Figure 3.8B). Without *PRR7*, transcription of *CCA1* and *LHY* are still sensitive to GDA, which indicated that *PRR7* was not the sole target of Hsp90. In GDA-treated *prr9*, transcription levels of *CCA1* and *LHY* remained the same as non-treated plants. This could be interpreted as PRR9 is a critical target of Hsp90, as GDA did not affect transcription of *CCA1* and *LHY* in the morning without PRR9 (Figure 3.8C, D). Not surprisingly, in *prr7 prr9*, there was no significant difference in transcription levels of *CCA1* and *LHY* in the morning, especially from ZT6 to ZT10 (Figure 3.8E, F). To summarize, the morning clock component PRR9 is a genetic target of Hsp90, whereas PRR7 could not be proved to be a target of Hsp90.

3.2.4 Clock period is related to transcription level of *CCA1* and *LHY*

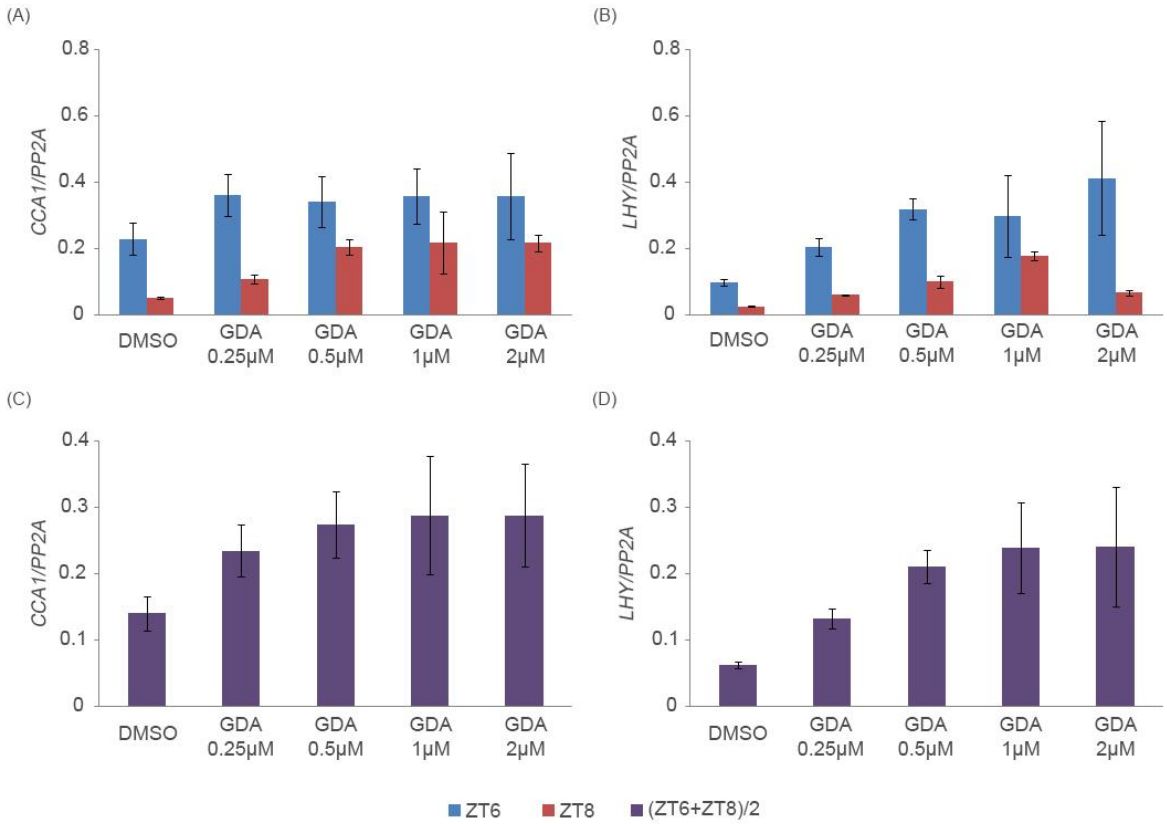

Figure 3.9 Accumulation of CCA1 and LHY are positively related with the concentration of GDA applied.

(A) and (B), accumulation of *CCA1* and *LHY* with GDA treatment at different concentrations (0.25μM, 0.5μM, 1μM and 2μM) at ZT6 (blue bar) and ZT8 (red bar), respectively. (C) and (D), averaged accumulation of *CCA1* and *LHY* at different concentration. The replicate samples were treated with GDA at different concentrations (0.25μM, 0.5μM, 1μM and 2μM) for two days. Samples were collected at ZT6 and ZT8. Expression values were normalized to *PP2A* and are representative of three biological replicates. Error bars indicate SD.

As GDA lengthened period (Figure 3.3) and raised accumulation of *CCA1* and *LHY* in the morning (Figure 3.6 C, D), my hypothesis was that period length was positively related to the accumulation of *CCA1* and *LHY* in morning. Time points ZT6 and ZT8 were selected to monitor the effect of GDA at different concentrations (0.25μM, 0.5μM, 1μM, and 2μM), because as shown, GDA resulted in the most significant effect at ZT6 and ZT8 (Figure 3.6C, D). When the concentration of GDA gradually increased from 0 to 2μM, accumulation of *CCA1* slightly increased at ZT6. However, at ZT8, accumulation of *CCA1* steadily increased with the increasing concentration of GDA. Compared to the amount at 0μM (DMSO), which is 0.05, the accumulated *CCA1* at 2μM reached 0.22, which is 4 times as much as that at 0μM (Figure 3.9A). To clarify the trend, I averaged the accumulation at ZT6 and ZT8. The accumulation of *CCA1* was positively related with concentration of GDA (Figure 3.9C). Accumulation of *LHY* was similar to *CCA1*. Although there was an unexpected decrease at ZT8 (2μM), the averaged amount showed the trend that accumulation of *LHY* increased with the increasing concentration of GDA (Figure 3.9 B, D). In parallel, period length was measured at different concentrations of GDA treatment. For both Col *LHY::LUC* and *GI::LUC*, the periods became longer when concentration of GDA gradually increased (Figure 3.10A, B). In conclusion, period length was positively related to the transcription levels of *CCA1* and *LHY* in the morning.

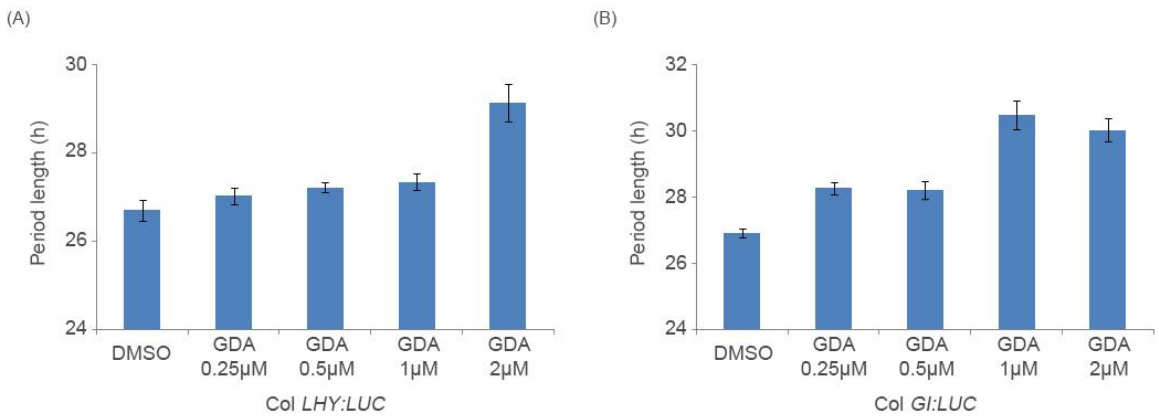

Figure 3.10 Period length increases with increasing concentration of GDA.

(A) Period length of Col *LHY:LUC* with GDA treatment at different concentrations. DMSO, 26.71±0.24h; 0.25μM, 27.03±0.19h; 0.5μM, 27.23±0.12h; 1μM, 27.35±0.18h; 2μM, 29.14±0.43h. (B) Period length of Col *GI:LUC* with GDA treatment at different concentrations. DMSO, 26.93±0.13h; 0.25μM, 28.27±0.19h; 0.5μM, 28.23±0.27h; 1μM, 30.49±0.42h; 2μM, 30.04±0.35h.Error bars indicate SEM, n=24.

3.2.5 GDA reduces the amount of ELF3

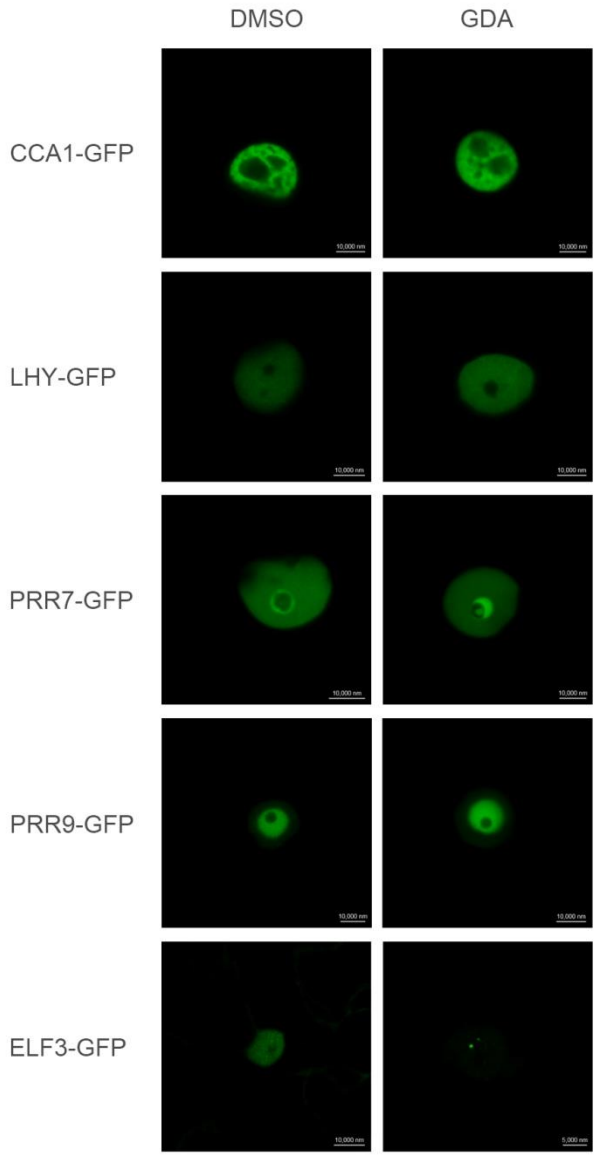

Figure 3.11 Protein amount of clock components after GDA treatment.

Confocal microscopy of *CCA1*, LHY, PRR7, PRR9, and ELF3 in *N. benthamiana*. All proteins tagged with GFP protein were expressed under the 35s promoter. The confocal microscopy experiment was performed 3 days after *Agrobacterium* being infiltrated, The images were generated 3 hours after 10μM GDA was injected into tobacco leaves. The left lane shows GFP signals after DMSO was injected, which served as a negative control. The right lane shows the GFP signal after GDA was injected.

As previously shown, GDA affected the circadian clock through morning genes. Therefore, I measured the protein amount of CCA1, LHY, PRR7, and PRR9 before and after GDA treatment to see if any of these were potentially controlled at the

protein level by Hsp90 action. In infiltrated tobacco leaf cells after 3-hour GDA treatment. GFP signals of CCA1-GFP and LHY-GFP remained the same, compared to those without GDA treatment. This indicates that Hsp90 is unlikely to directly control the amount of CCA1 and LHY at the protein level. The qRT-PCR data suggested that GDA alters gene accumulation of *CCA1* and *LHY* through PRR9 (Figure 3.8C-F). However, protein accumulation of PRR7 and PRR9 were also not affected by GDA (Figure 3.11). As such, the regulator of PRR9 and PRR7 could be a protein target.

As demonstrated, gene accumulation of *PRR9* was altered by GDA (Figure 3.7B). I next focused on examining its transcriptional regulator ELF3. Since ELF3 binds to the *PRR9* promoter to repress its expression (Eva *et al*., 2012), my hypothesis was that GDA altered gene accumulation of *CCA1*, *LHY*, and *PRR9* through an ELF3 cascade. Therefore, I next examined if GDA affects the protein amount of ELF3. The image showed that after GDA was injected into tobacco leaves, the fluorescent signal of GFP-tagged ELF3 was significantly reduced, compared to the non-GDA treated cells. In conclusion, GDA reduces ELF3 protein, which implicates that Hsp90 activity in stabilizing ELF3 levels. This might result in the alteration of gene accumulation of *PRR9*, which subsequently result in alterations of gene accumulation of *CCA1* and *LHY*.

3.2.6 ELF3 is co-localized with Hsp90.2

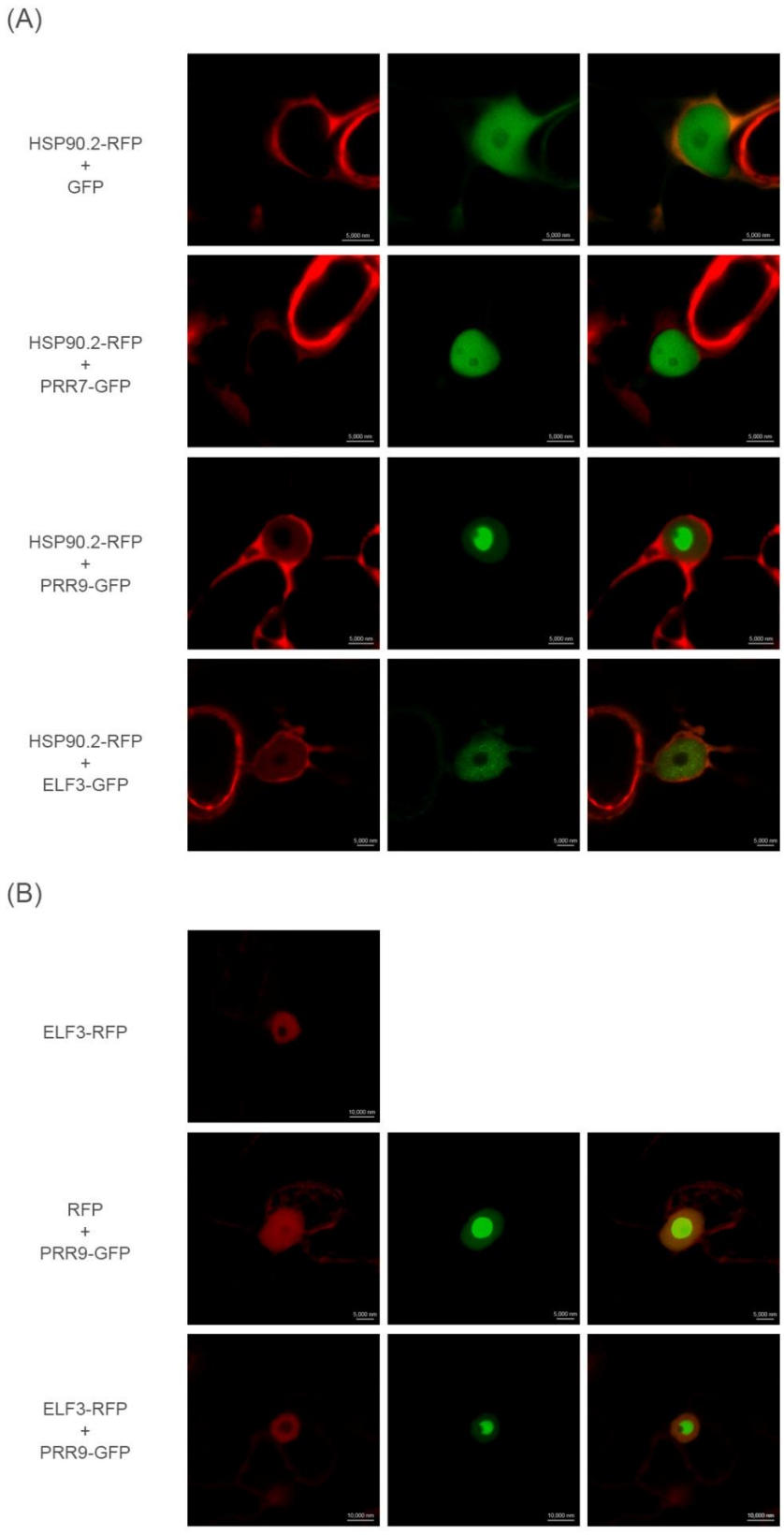

Figure 3.12 ELF3 is co-localized with Hsp90.2.

(A) Confocal microscopy of Hsp90.2-RFP versus PRR7-GFP, PRR9-GFP and ELF3-GFP in *N. benthamiana*. (B) Confocal microscopy of ELF3-RFP versus PRR9-GFP in *N. benthamiana*. All proteins were expressed under the 35S promoter. The images were generated 3 days after co-infiltration. From left to right in (A) and (B), they were RFP channel, GFP channel and GFP/RFP mixed channel.

As GDA is a specific inhibitor of Hsp90, the reduction of ELF3 after GDA treatment (Figure 3.11) suggested that ELF3 was likely to be a target of Hsp90. To identify if ELF3 and Hsp90.2 physically interact with each other, I co-expressed Hsp90.2 and ELF3. Meanwhile, I co-expressed PRR7 and PRR9, since it was shown that PRR9 is a potential target of Hsp90 (Figure 3.8). When Hsp90.2-RFP was co-expressed with GFP as a negative control, the fluorescent signal only existed in the cytoplasm and no signal was detected in the nucleus. When Hsp90.2-RFP was co-expressed with PRR7-GFP, Hsp90.2 was still in the cytoplasm while PRR7 was expressed only in the nucleus. This shows there is no overlap between Hsp90.2 and PRR7. When Hsp90.2-RFP was co-expressed with PRR9-GFP, Hsp90.2 appeared both in the cytoplasm and in the nucleus. PRR9 was highly focused in the center of the nucleus with relatively low accumulation around the outer ring. Interestingly, after co-expression, the Hsp90.2 was not homogeneously localized in the nucleus, but was focused in PRR9's outer ring area, which indicates that there is an overlap in accumulation. When Hsp90.2-RFP was co-expressed with ELF3, both ELF3 and Hsp90.2 appear in both the cytoplasm and nucleus, which shows that ELF3 relocates some Hsp90.2 proteins into the nucleus. In both the nucleus and the cytoplasm, there was an exact overlapping between ELF3 and Hsp90.2 (Figure 3.12A).

To answer why Hsp90.2 appeared only in the outer ring area of PRR9 in the nucleus when Hsp90.2 and PRR9 were co-expressed, I co-expressed ELF3-RFP and PRR9-GFP. The results showed that ELF3 also appeared in the PRR9 outer ring area only. This is quite different from the single ELF3-RFP expression and PRR9-GFP co-expression with RFP, in which the RFP signals homogeneously existed in the nucleus (Figure 3.12B). According to Figure 3.12A and B, Hsp90.2 and ELF3 exactly overlapped with each other. In conclusion, ELF3 relocated the Hsp90.2 to the nucleus

and had a co-localization with Hsp90.2, which indicated that there might be a physical interaction between ELF3 and Hsp90.2.

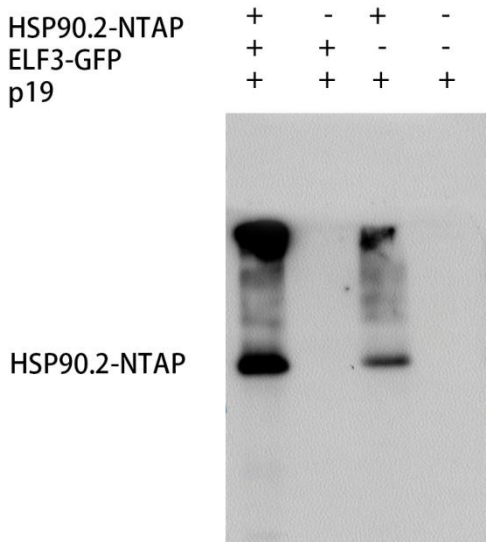

Figure 3.13 ELF3 can bind with Hsp90.2 *in vivo*.

The Co-immunoprecipitation assay showed that ELF3 could physically bind to Hsp90.2 *in vivo*. Agrobacteria carrying two target plasmids to express ELF3 and Hsp90.2 were injected into tobacco leaves. After three days, the leave sample was collected and proteins were extracted. The N-terminal GFP tagged ELF3 was pulled down by the GPF trap beads and the N-terminal N-TAP tagged Hsp90.2 was detected by western blot.

ELF3 was able to bind to Hsp90.2 in tobacco. In the first lane, the sample contained both N-TAP-tagged Hsp90.2 and GFP-tagged ELF3. When ELF3 was pulled down by GFP trap beads, Hsp90.2 was also pulled down together and could be detected by western blot. In the second lane, the sample did not contain Hsp90.2 protein. Therefore, although ELF3 was pulled down, there is no Hsp90.2 signal on the film. In the third lane, the sample lacked of ELF3 protein. However, Hsp90.2-GFP signals were detectable. The reason might be that the huge amount of Hsp90.2 in the sample could unspecifically bind to the GFP trap beads. Therefore, some GFP signals could be detected. In the fourth lane, neither ELF3 nor Hsp90.2 was included and there was no signal detected. To conclude, ELF3 and Hsp90.2 could physically interact with each other *in vivo*, indicating that ELF3 might be a direct target of Hsp90.

3.3 Discussion

In this chapter, I showed that Hsp90 was involved in the temperature-regulation of the *Arabidopisis* circadian clock. Hsp90 indirectly affected gene accumulation of *CCA1* and *LHY* through PRR9, which resulted in the changing of clock period length. Moreover, Hsp90 could directly interact with ELF3, and this involves redirection of PRR9 protein as well. ELF3 were shown to be an upstream regulator of *PRR9* (Herrero et al., 2012; Thines and Harmon, 2010). Therefore, Hsp90, one of the most important protein chaperons, might affect the *Arabidopsis* circadian clock sequentially through ELF3, PRR9, and CCA1/LHY.

The effect of Hsp90 on clock period length was examined under both light-dark and warm-cold entrainment conditions (Figure 3.1). Under both conditions, the *hsp90.2-3* mutants showed a longer period than the Ws wild type, which suggested that Hsp90 was involved in both light- and temperature-regulation. However, the lengthening effect caused by *hsp90.2-3* mutation was more significant when seedlings were entrained under warm-cold condition. Since the light and temperature pathway were partially independent, Hsp90 is likely not only involved in the common signaling pathway shared by light and temperature but also specifically involved in the independent temperature signaling pathway.

As a specific inhibitor of Hsp90, GDA treatment on the seedlings resulted in longer period phenotypes in both Ws and Col background (Figure 3.2 and Figure 3.3). The lengthening effect of GDA was even stronger than the *hsp90.2-3* mutation. Since Hsp90 has several isoforms in Arabidopsis, as long as the concentration was high enough, GDA results in ATP-binding defects in all Hsp90s, whereas *hsp90.2-3* mutation only altered the ATP-binding site of Hsp90.2. Therefore, it was reasonable that GDA could strongly lengthen the period by inhibiting more Hsp90s. In addition, GDA could also dampen bioluminescence signals and the reduce robustness of circadian clock (Figure 3.2 and Figure 3.3). This might be due to the ATP-binding defects of Hsp90 (Whitesell et al., 1992). Furthermore, Col wild type was more sensitive to GDA, as the period differences between GDA-treated and non-GDA-treated seedlings were larger compared the differences in Ws wild type, which suggested that Col might be more sensitive to stress condition due to its sensitivity to

the defects of Hsp90. As a conclusion, it was again demonstrated that Hsp90 was involved in the thermal regulation of the clock.

The phase response curve assay revealed that Hsp90.2 influenced the clock response to heat shock stress before dawn. The differences in phase shift were only observed at ZT(-3) and ZT0, which suggested that Hsp90 could affect the circadian clock by interacting with the late-evening or early-morning clock components. It is consistent with previously published results, which showed that Hsp90 can influence the clock through three evening components TOC1, GI and ZTL (Kim et al., 2011). Therefore, I tested all the potential targets of Hsp90.

GDA resulted in different period phenotypes in the different clock mutants. The *cca1*, *lhy*, and *toc1* single mutants maintained a similar period length after GDA treatment. The period was even shorter for *cca1 lhy* double mutant (Figure 3.5), indicating that these three clock components were potential targets of Hsp90. Consistently, CCA1, LHY and TOC1 were previously identified to be involved in temperature regulation (Gould et al., 2006; Salome et al., 2010). In addition, the periods of both *elf3* and *gi* mutants were lengthened by GDA, indicating that *ELF3* and *GI* transcripts were not the targets of Hsp90. This does not preclude these as protein targets. However, previous findings showed that both ELF3 and GI are the key components in temperature regulation processes (Gould et al., 2006; Thines and Harmon, 2010). This point will be discussed later in the final chapter.

The gene accumulation patterns showed that as potential targets of Hsp90, the gene expression of *CCA1* and *LHY* were not affected by GDA under light-dark entrainment while their expression patterns were altered under warm-cold entrainment condition (Figure 3.6). This set of results suggested that in light-regulation pathway *CCA1* and *LHY* were not targets of Hsp90. In addition, the alteration in expression of *CCA1* and *LHY* indicates that *CCA1* and *LHY* are the indirect targets of Hsp90 in temperature-regulation pathway. Interestingly, the influence of Hsp90 on gene accumulation of *CCA1* and *LHY* was PRR9-dependent. In the *prr9*, the gene accumulation pattern was not affected by GDA (Figure 3.8). PRR9 was demonstrated to be one of the transcriptional repressor of *CCA1* and *LHY* (Nakamichi et al., 2010; Nakamichi et al., 2005). Therefore, PRR9 is proposed to be

one component in the Hsp90 regulation, downstream of Hsp90 and upstream of *CCA1* and *LHY*.

In Figure 3.9 and 3.10, I linked gene expression levels to period length. When the expression of *CCA1* and *LHY* increased at ZT6 and ZT8, the period lengths also increased gradually. Although expression of *CCA1* and *LHY* in GDA-treated plant was lower than non-treated at peak times (Figure 3.6), period was lengthened due to the relatively higher expression late in the morning. This indicates that period length was not determined by the peak expression amount of *CCA1* and *LHY*, whereas it was somehow determined by the width of the time window of expression above certain level. To conclude, Hsp90 lengthens period by raising expression in the morning and thus lengthening the effective-expression time window.

GDA reduced ELF3 protein amount, instead of CCA1, LHY, PRR7, and PRR9 (Figure 3.11). In addition, Hsp90.2 co-localized with ELF3 in both nucleus and cytoplasm (Figure 3.12). Furthermore, *in vivo* protein binding assay demonstrated that Hsp90.2 physically interacted with ELF3 (Figure 3.13). These results filled the gap between PRR9 and Hsp90.2. ELF3 was demonstrated to repress *PRR9* by binding to its promoter (Herrero et al., 2012). Also, the increase of PRR9 and PRR7 by thermal induction was eliminated in the *elf3-1* mutant (Thines and Harmon, 2010). Therefore, as the upstream regulator of PRR9, ELF3 was considered as the direct target of Hsp90, mediating the regulation of Hsp90 on the circadian clock. Further discussion would be in the final chapter.

Chapter 4 Allele specific actions of Hsp90.2 on the clock

4.1 Introduction

Alleles of Hsp90.2 beyond *hsp90.2-3* were previously reported. These include *hsp90.2-1* (G95E), *hsp90.2-4* (S100F), *hsp90.2-6* (A42T), *hsp90.2–7* (A11T) and *hsp90.2-8* (R337C). Here these alleles were examined for clock phenotypes.

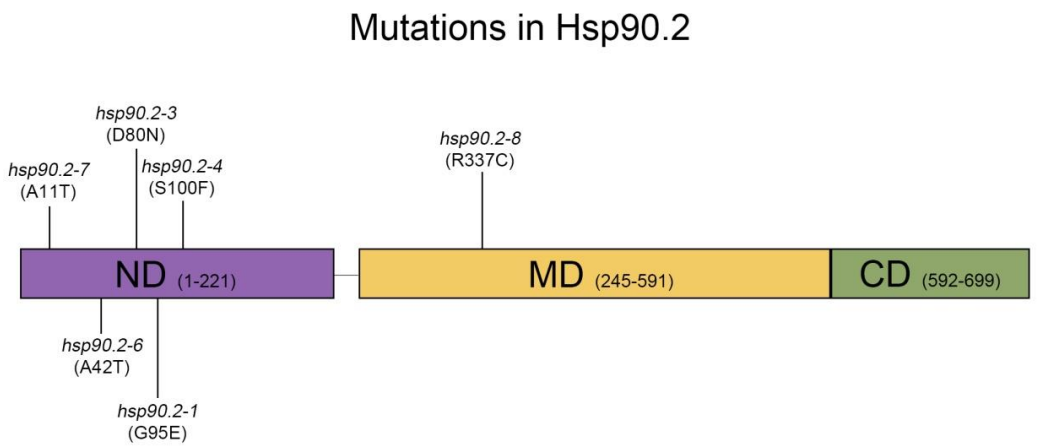

Figure 4.1 Point mutations in Hsp90.2.

Hsp90 contains three domains: an N-terminal conserved ATP-binding domain, a middle domain, and a C-terminal dimerization domain. Six point mutations are included: *hs90.2-1* (G95E), *hsp90.2-3* (D80N), *hsp90.2-4* (S100F), *hsp90.2-6* (A42T), *hsp90.2-7* (A11T), and *hsp90.2-8* (R337C).

hsp90.2-1 (G95E) is adjacent to residues making contact with ATP. The G95E change alters the local charge density (David A. Hubert, 2003). *hsp90.2-3* (D80N) alters a residue previously shown to make multiple ATP contacts in the crystal structure of yeast Hsp90 (Prodromou et al., 1997). The *hsp90.2-4* (S100F) is adjacent to residues making direct contact with ATP, resulting in the addition of a large hydrophobic side chain (David A. Hubert, 2003). *hsp90.2–7* encodes an A11T change at the N-terminal strand of an Hsp90 protein. *hsp90.2–8* encodes a R337C change at the middle domain physically adjacent to the ATPase domain in the closed conformation of Hsp90 dimer. The *hsp90.2–8* mutation (R337C) exhibits a nearly full loss of ATPase activity (Figure 4.1).

To identify the influence of these *hsp90.2* mutations on the clock, and subsequently reveal the different functions of Hsp90, I crossed the *hsp90.2* mutants

with *GI::LUC*-containing Col-0 and screened the homozygous lines for periodicity analysis. Differentiated phenotypes were detected.

4.2 Results

4.2.1 Light-entrained Hsp90.2 mutants

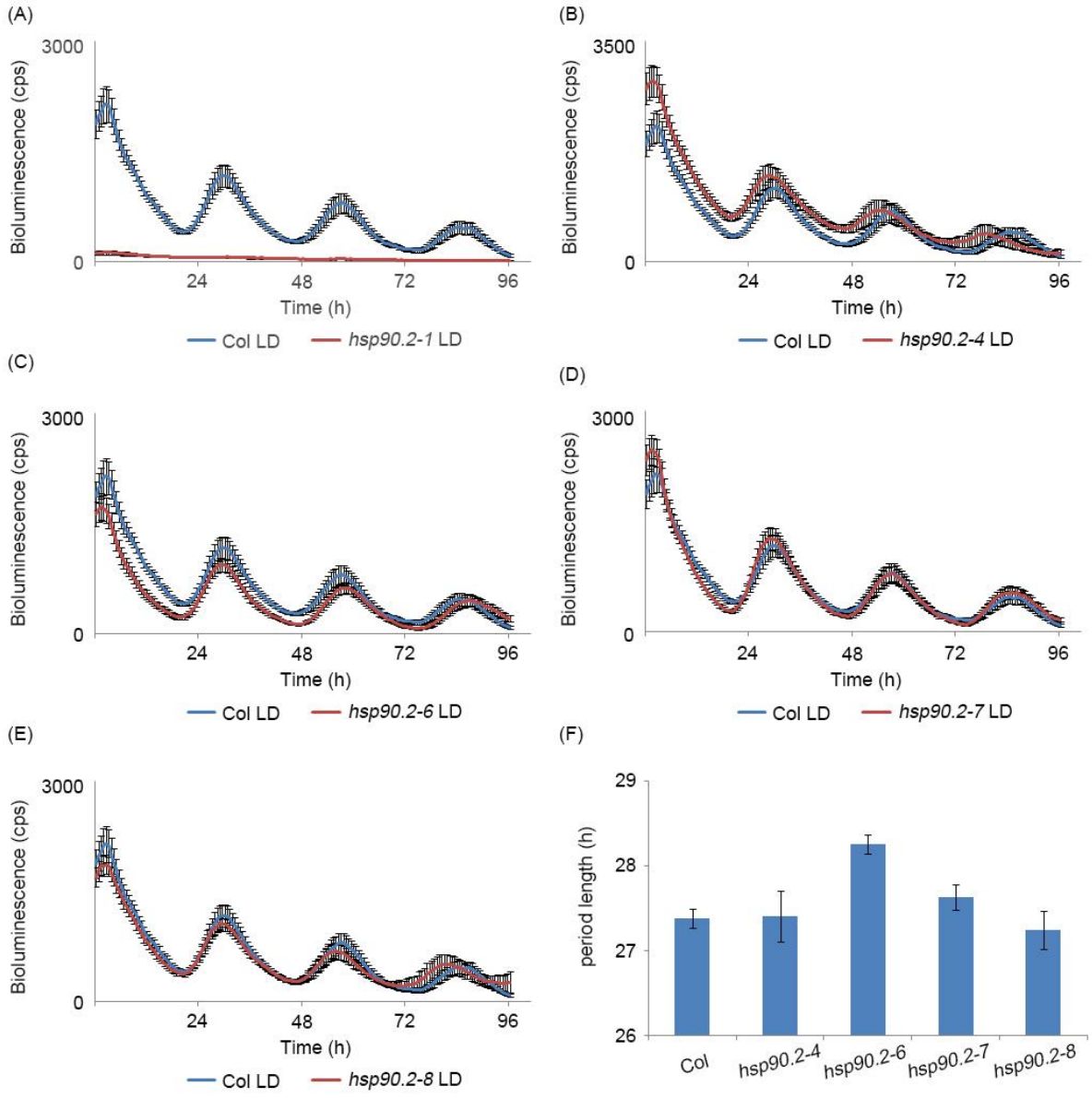

Figure 4.2 *hsp90.2* mutations resulted in different period phenotypes under LD condition.

(A) Bioluminescence of *GI:LUC* in *hsp90.2-1* mutant; (B) Bioluminescence of *GI:LUC* in *hsp90.2-4* mutant; (C) Bioluminescence of *GI:LUC* in *hsp90.2-6* mutant; (D) Bioluminescence of *GI:LUC* in *hsp90.2-7* mutant; (E) Bioluminescence of *GI:LUC* in *hsp90.2-8* mutant. (F) Period length of Col, *hsp90.2-4, hsp90.2-6, hsp90.2-7* and *hsp90.2-8.* Col, 27.38±0.11h; *hsp90.2-4*, 27.41±0.30h; *hsp90.2-6*, 28.26±0.11h; *hsp90.2-7,* 27.63±0.15h; *hsp90.2-8,* 27.25±0.23h. The blue curve in (A)-(E) is Col GI:LUC. All lines were entrained under LD condition. Error bars indicate SEM, n=48. LD = light-dark.

To identify the effect on the circadian clock resulting from different mutations in the Hsp90.2 protein, I crossed the respective *hsp90.2* alleles to Col *GI:LUC* plants and screened the homozygous lines to measure their period length after entrainment. First, I phenotyped these plants under light-dark entrainment conditions. The *hsp90.2-1* bioluminescence signal was significantly lower. Perhaps the luciferase reporter was silenced. However, the original data showed that the bioluminescence signal was at normal strength before the free-running period started. This indicated that the low signal strength was conditional (Figure 4.2A). A shorter period length was observed in the rhythmic curve for *hsp90.2-4* (Figure 4.1B). However, the period length remained the same as Col wild type (Figure 4.2F). For *hsp90.2-6*, period length was significantly longer than that of Col wild type (Figure 4.2C, F). For *hsp90.2-7*, the period was slightly longer compared to the wild type (Figure 4.2D, F). For *hsp90.2-8*, the period was slightly shorter than wild type, which is more obvious in the rhythmic curve chart (Figure 4.2 E, F). In conclusion, beside *hsp90.2-1*, which had a dampened bioluminescence signal, another two alleles, *hsp90.2-4* and *hsp90.2-8*, had no significant period difference compared to wild type. In contrast, *hsp90.2-6* and *hsp90.2-7*, had a longer period than the wild type.

4.2.2 Temperature-entrained Hsp90.2 mutants

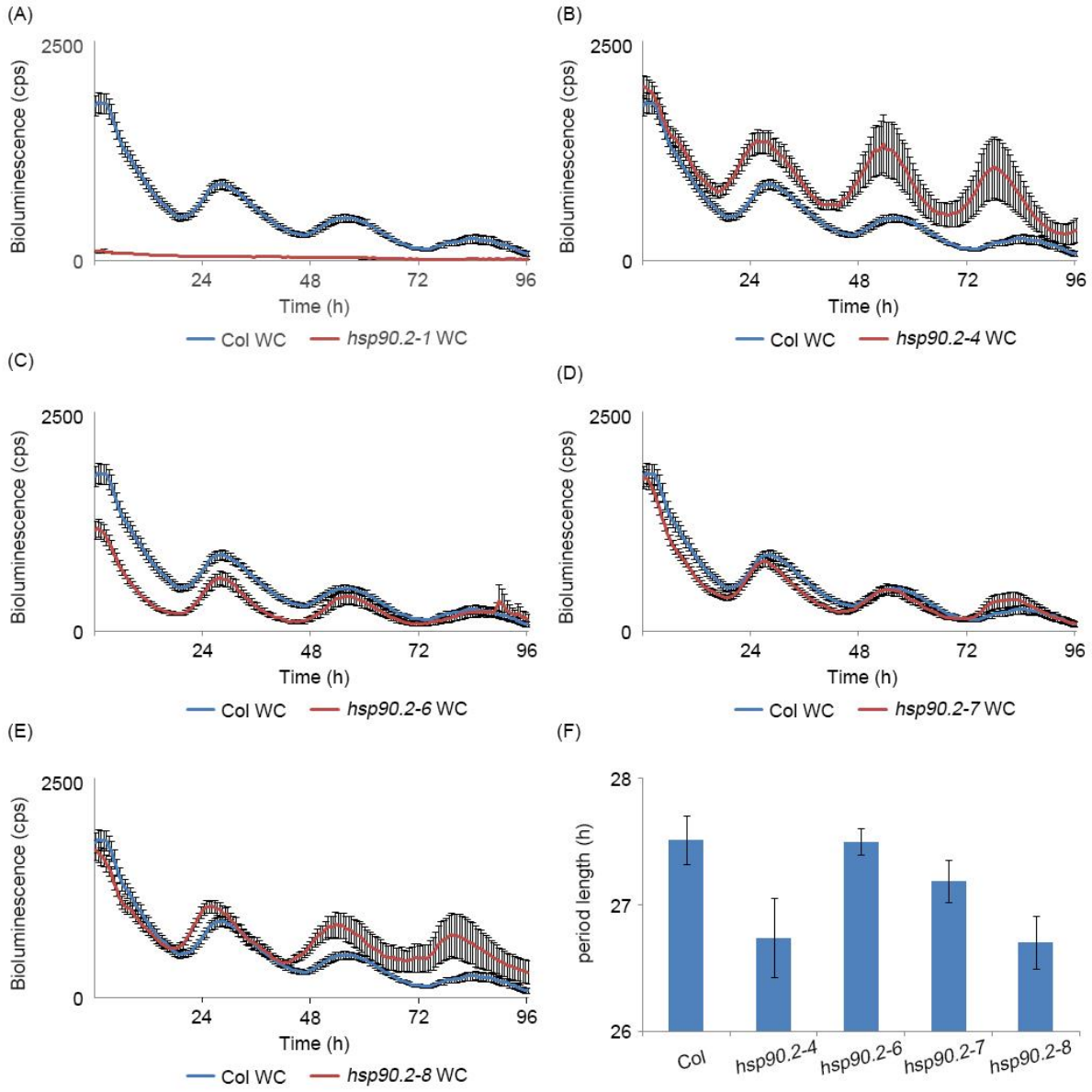

Figure 4.3 *hsp90.2* mutations resulted in different period phenotypes under WC condition.

(A) Bioluminescence of *GI:LUC* in *hsp90.2-1* mutant; (B) Bioluminescence of *GI:LUC* in *hsp90.2-4* mutant; (C) Bioluminescence of *GI:LUC* in *hsp90.2-6* mutant; (D) Bioluminescence of *GI:LUC* in *hsp90.2-7* mutant; (E) Bioluminescence of *GI:LUC* in *hsp90.2-8* mutant. (F) Period length of Col, *hsp90.2-4, hsp90.2-6, hsp90.2-7* and *hsp90.2-8.* Col, 27.52±0.19h; *hsp90.2-4*, 26.74±0.31h; *hsp90.2-6*, 27.50±0.10h; *hsp90.2-7,* 27.19±0.17h; *hsp90.2-8,* 26.71±0.21h. The blue curve in (A)-(E) is Col GI:LUC. All lines were entrained under WC condition. Error bars indicate SEM, n=48. WC = warm-cool.

Hsp90 is associated to the temperature signaling pathway, as demonstrated in Chapter 3. I thereby measured the additional alleles period length under warm-cold entrainment condition. As in the light-dark condition, *hsp90.2-1* has a dampened bioluminescence signal was dampened (Figure 4.3A). For *hsp90.2-4*, the period was significantly shortened (Figure 4.3B, F). *hsp90.2-6* had no period change compared to Col wild type (Figure 4.3C, F). For *hsp90.2-7*, according to the bar chart, the period was slightly shortened compared to the Col wild type (Figure 4.3D, F). The period of *hsp90.2-8* was significantly shortened, as was *hsp90.2-4* (Figure 4.3E, F). In conclusion, *hsp90.2-1* again had a dampened bioluminescence signal. *hsp90.2-4* and *hsp90.2-8* had a much shorter period compared to the Col wild type. *hsp90.2-7* had a slightly shorter period phenotype, while the period length of *hsp90.2-6* remained the same as the Col wild type.

4.3 Discussion

In this chapter, I identified that the examined alleles of *hsp90.2* resulted in different period phenotypes. After light-dark entrainment, *hsp90.2-6* and *hsp90.2-7* mutations resulted in a longer period (Figure 4.2), while under warm-cold condition, *hsp90.2-4* and *hsp90.2-8* mutations resulted in a shorter-period phenotype (Figure 4.3). Therefore, the diverged period phenotype suggested that Hsp90 affects the circadian clock in various ways.

Including previously mentioned *hsp90.2-3* (D80N) in chapter 3, most of the *hsp90.*2 mutation I studied are located in the N-terminal ATP-binding domain (Figure 4.1), with the exception of *hsp90.2-8*, which was located in the middle domain. Interestingly, according to both the period phenotypes and the location sites of the mutations, *hsp90.2* could be divided into two groups. The first three mutations located at the beginning of N-terminal site, including *hsp90.2-7* (A11T), *hsp90.2-6* (A42T) and *hsp90.2-3*(D80N) caused a longer period phenotype. However, *hsp90.2-4* (S100F) and *hsp90.2-8* (R337C) were the last two mutations, causing a shorter period phenotype.

Interestingly, although the mutations similarly cause the reduction of ATPase activity, they resulted in different clock phenotypes. Both *hsp90.2-7* (A11T) and *hsp90.2-8* (R337C) destabilize the lid-closed conformation. As previously demonstrated, the lid-closed conformation is important for ATPase activity of Hsp90 (Ali et al., 2006). Moreover, the two mutations reduce Hsp90-ND dimer formation *in vitro* (Hubert et al., 2009). However, the two mutations resulted in different period phenotypes. Furthermore, as shown in Chapter 3, GDA also resulted in a longer period, the same as the *hsp90.2-3*, *hsp90.2-6*, and *hsp90.2-7* while *hsp90.2-4* and *hsp90.2-8* resulted in shorter periods. Therefore, in addition to reducing ATPase activity, *hsp90.2-4* and *hsp90.2-8* should have other functions in clock regulation.

One possible interpretation is that *hsp90.2-8* causes defects in substrate binding. Hsp90 can assist the folding, stabilization and activation of various substrate proteins, including kinases and transcription factors involved in signal transduction and regulatory processes (Jackson et al., 2004; Krukenberg et al., 2011; Milioni and Hatzopoulos, 1997; Pratt et al., 2004). Importantly, the middle domain of Hsp90 plays

a key role in binding to substrate (Jackson et al., 2004). The *hsp90.2-8* mutation may alter the structure of the protein binding site. Thus, this alteration may affect the folding or stabilization of clock transcription factors, such as CCA1, LHY, and ELF3. Similarly, the *hsp90.2-4* mutation site might physically adjacent to the binding sites of the substrate proteins. The additional hydrophobic side chain may interfere the binding of substrate proteins.

Since *hsp90.2-4* and *hsp90.2-8* resulted in shorter periods, instead of the longer period phenotype of *hsp90.2-x*, which was thought to be caused by the reduction of ATPase activity, the proposed defects of substrate protein binding should be more dominant. The reason could be that Hsp90.2 is specifically recruited by some transcription factors involved in clock regulation while reduced ATPase activity can be made up by other Hsp90s.

In conclusion, Hsp90 may be involved in the regulation of the circadian clock in at least two ways. One is possible to be ATP-dependent, as once the ATPase activity of Hsp90 was reduced, the clock period was lengthened. The other might be directly binding to its client proteins to assist their folding, stabilization, and activation. This could relate to the short period effects after thermal entrainment.

Chapter 5 Final discussion and perspectives

5.1 Final discussion

5.1.1 ELF3 and GI collaborate in thermal signal input pathway

I identified that the *hsp90.2-3* mutant and GDA-treated seedlings showed a longer period phenotype (Figure 3.1 and 3.2). I further identified ELF3 is one client of Hsp90. Once Hsp90.2 in the cell was inhibited by GDA, the amount of ELF3 was reduced (Figure 3.11, 3.12, and 3.13). Transcription levels of *PRR7* and *PRR9* were not significantly elevated by GDA treatment (Figure 3.7). However, it was demonstrated that ELF3 is the transcription repressor of *PRR9*. In the *elf3* mutant, the gene accumulation level of *PRR9* was elevated. Meanwhile, the period of weak alleles of *elf3* was shortened (Kolmos et al., 2011). In addition, the *gi* mutant was still influenced by GDA. However, it has been proposed that Hsp90 influences the clock through ZTL, a downstream protein regulated by GI. Hsp90 and GI are tightly connected in the ZTL-stabilization, as the low levels of ZTL in *gi* mutant is not significantly reduced by GDA, which suggests that GDA should not result in a longer period in the *gi* mutant (Kim et al., 2007).

To explain these conflicts, I propose that both ELF3 and GI are involved in the temperature input pathway. These two components may be involved in two partially independent pathways. ELF3 and GI influence transcription of *CCA1* and *LHY* in opposite ways. ELF3 represses the transcription of *PRR9* whereas PRR9 represses the transcription of *CCA1* and *LHY* (Herrero et al., 2012; Nakamichi et al., 2005). Therefore, in theory, ELF3 positively regulates the transcription of *CCA1* and *LHY*. However, GI was demonstrated to positively regulate the transcription of *CCA1* and *LHY*. The *gi* mutations result in a reduction in the expression of *CCA1* and *LHY* (Fowler et al., 1999). Meanwhile, the *gi* mutants cause a short-period phenotype (Park et al., 1999). Interestingly, the nighttime repressor ELF3-ELF4-LUX negatively regulates the transcription of *GI* (Mizuno et al., 2014). Thus, the accumulation level of *CCA1* and *LHY* may reach the balance between the regulations of ELF3 and GI. In conclusion, Hsp90 influences the circadian clock through both ELF3 and GI, and ELF3 and GI are involved in partially independent pathways.

5.1.2 PRR9 and CCA1 may serve as stress indicators

Under normal conditions, Hsps are mainly located in the cytoplasm. However, under stress conditions, Hsps rapidly transfer to the nucleus (Horwitz, 1992; Lindquist and Craig, 1988). When HS90.2 was expressed alone in tobacco cells, it was found in the cytoplasm. However, Hsp90.2 was co-expressed with *35s::PRR9*, some Hsp90.2 transferred to the nucleus (Figure 3.12A), which suggested that accumulation of PRR9 may be recognized as a signal of stress.

The gene accumulation of *PRR9* was elevated in warm conditions (Mizuno et al., 2014). Considering this point, it is reasonable to match the expression of *PRR9* to the daily cycle. Normally, temperature increases from early morning to the middle of the day. Meanwhile, expression of *PRR9* gradually increases in the morning and reaches its peak level in the middle of the day. The oscillation of *PRR9* accumulation perfectly matches the daily rhythmic changes of temperature. The average accumulation level of PRR9 may match the seasonal changes, as in summer the average level of *PRR9* would be higher than that in winter. Therefore, my hypothesis is that PRR9 could serve as a “thermometer” which tells the plant the temperature. Overexpression of PRR9 may mislead the plant in sensing the actual temperature, simulating a heat stress and triggering stress responses, which is like a “fever”.

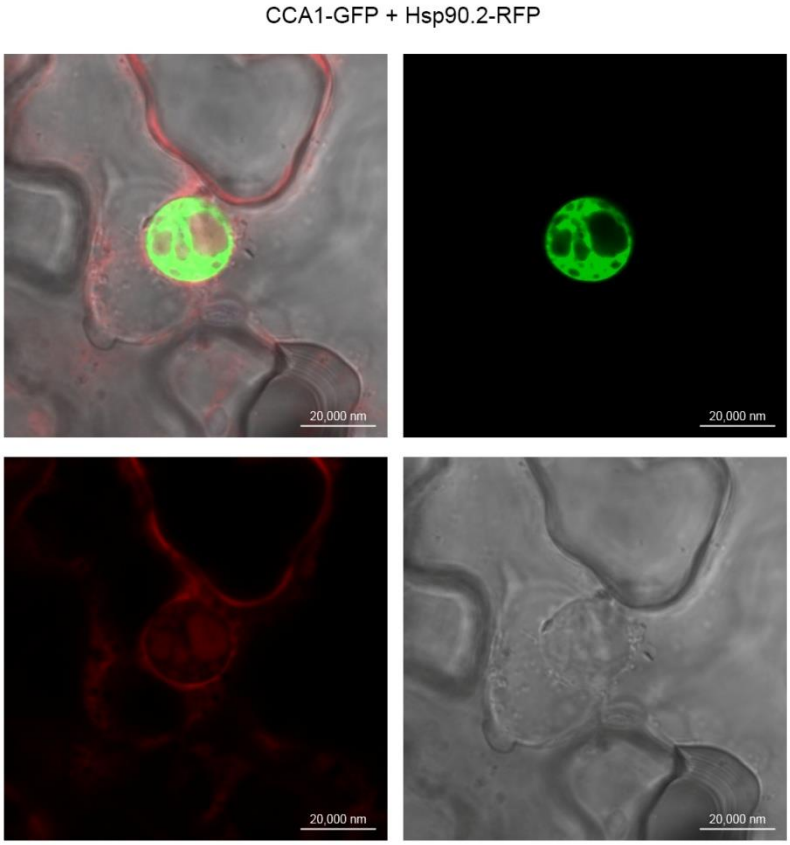

Figure 5.1 CCA1-GFP is co-expressed with Hsp90.2-RFP in *N. benthamiana.*

When CCA1 was highly expressed in the nucleus, Hsp90.2 transferred into nucleus but is not completely co-localized with CCA1. The green channel is GFP tagged CCA1. The red channel is RFP tagged Hsp90.2

CCA1 may be also recognized as another stress indicator. Hsp90.2 transferred to the nucleus when CCA1 was highly expressed (Figure 5.1). It appears that CCA1 was involved in the biotic stress regulation pathway. When I injected transformed *agrobacteria* with several clock constructs into tobacco leaves, only the *Agrobacterium* containing *35s::CCA1* resulted in a severe infection, which might indicate that CCA1 is involved in the plant immune system. However, it was previously demonstrated that CCA1 controls the expression of defense genes and timing of the immune response. The *cca1* mutant showed compromised resistance whereas the CCA1-overexpression line showed enhanced resistance (Wang et al., 2011). This is completely opposite to my observation. One explanation is that the exogenous CCA1 strongly competes with native CCA1 in tobacco, which heavily interfere with the CCA1 immune regulation pathway, resulting in higher susceptibility

to pathogens. If considering the low expression level of *CCA1* at higher temperature, there should be a “clock-temperature-immune triangle” in *Arabidopsis*.

5.1.3 Temperature alters the functions of evening complex ELF3-ELF4-LUX

CCA1, LHY, PRR7, PRR9, and GI respond to a temperature upshift only during the dark period. The transcription of these genes were regulated by the evening complex (EC) night repressor ELF3-ELF4-LUX. A warmer temperature inhibits EC function, whereas a cooler temperature stimulates its function (Mizuno et al., 2014).

It is still unclear whether DNA-binding of EC to the target promoters is inhibited by a warm temperature or a warm temperature inhibits the repressor ability of EC. Considering the role of Hsp90, it can either regulate the protein stability of ELF3 or correct formation of EC. When Hsp90 is not sufficient to stabilize the proteins, the ability of EC may be inhibited under a warm condition.

5.1.4 Hypothesis on CCA1/LHY-PRR7/PRR9 self-balancing loop

CCA1/LHY activates transcription of *PRR7*/*PRR9* whereas PRR7 inhibits transcription of *CCA1*/*LHY* (Nakamichi et al., 2005). When the accumulation of *CCA1* and *LHY* were reduced from ZT20 to ZT2 by GDA, the accumulation of *PRR7* and *PRR9* also increased at a slower pace (Figure 3.6 and 3.7). After ZT4, the lower accumulation of PRR7 and PRR9 in GDA-treated seedlings did not inhibit *CCA1* and *LHY* as much as in the non-treated seedlings. Therefore, the accumulation of *CCA1* and *LHY* became relatively higher after ZT4. Meanwhile, expression of *PRR7* and *PRR9* after ZT10 was also elevated, which might be due to the higher amount of CCA1 and LHY. It was noted that the expression peaks of CCA1/LHY and PRR7/PRR9 were all shifted (Figure 3.6 and 3.7).

As mentioned in the discussion part of Chapter three, the effective expression window of *CCA1*/*LHY* was widened by GDA, which may explain the long period phenotype. In fact, less active Hsp90 may make the clock more sensitive to temperature. GDA may degrade clock-related components at 22°C as fast as that at 30°C, and thus switched the seedlings into a “summer state”. Based on this hypothesis, the wider effective expression window of *CCA1*/*LHY* matches the long-day conditions in summer. In summer conditions, temperature typically reaches its

peak around 2 p.m., which is around 8 hours after dawn. This point matches the shifted expression pattern of *PRR7*/*PRR9*.

In summary, my hypothesis is that the CCA1/LHY-PRR7/PRR9 morning loop model may tell us how the plant anticipates the daily rhythmic changes in different seasons.

5.1.5 three-layer clock model

So far, developed mathematical models consist of the core loop, the morning loop and the evening loop. However, one question remains to be answered: which component contributes more to the clock? Here I propose a modified model, in which the clock components are classified into three hierarchies.

The first layer (inner layer) contains three core components: CCA1, LHY, and TOC1 (Figure 5.2). These three components define the “clock”. These three genes are notably crucial, as in the *cca1 lhy toc1* triple mutant, the clock stays arrhythmic (Green and Tobin, 1999; Mizoguchi et al., 2002). Moreover, overexpression of either *CCA1* or *LHY* causes arrhythmicity of the clock (Schaffer *et al*., 1998; Wang and Tobin, 1998). The second layer (middle layer) contains the “adjusters” (Figure 5.2). The signal receivers are the outputs of clock. They form interlocked loops with core components, which reciprocally regulate each other. Once they receive the signals from the third layer (outer layer), their own expression or function are altered. They form interlocked loops with core clock components, thus the core clock is finely adjusted. PRR7 and PRR9 are two of the adjusters. The *prr7*, *prr9*, and the double mutant *prr7 prr9*, make the clock slower (Alabadi *et al*., 2001; Farre *et al*., 2005; Yamamoto *et al*., 2003). In addition, the *prr7-3 prr9-1* double mutant is not able to be reset by temperature pulses (Salome and McClung, 2005; Salome et al., 2010). The third layer (outer layer) contains the “signal mediators” (Figure 5.2). The signal mediators interact with the signal receivers to complete the signal transduction. The signal mediators do not have to be clock outputs. ELF3 may be one of the mediators. The repressing efficiency of ELF3 on *PRR7* and *PRR9* changes at different temperatures (Mizuno et al., 2014). The temperature induction of *PRR7* and *PRR9* mRNA accumulations were eliminated in the *elf3-1* mutant. (Thines and Harmon, 2010).

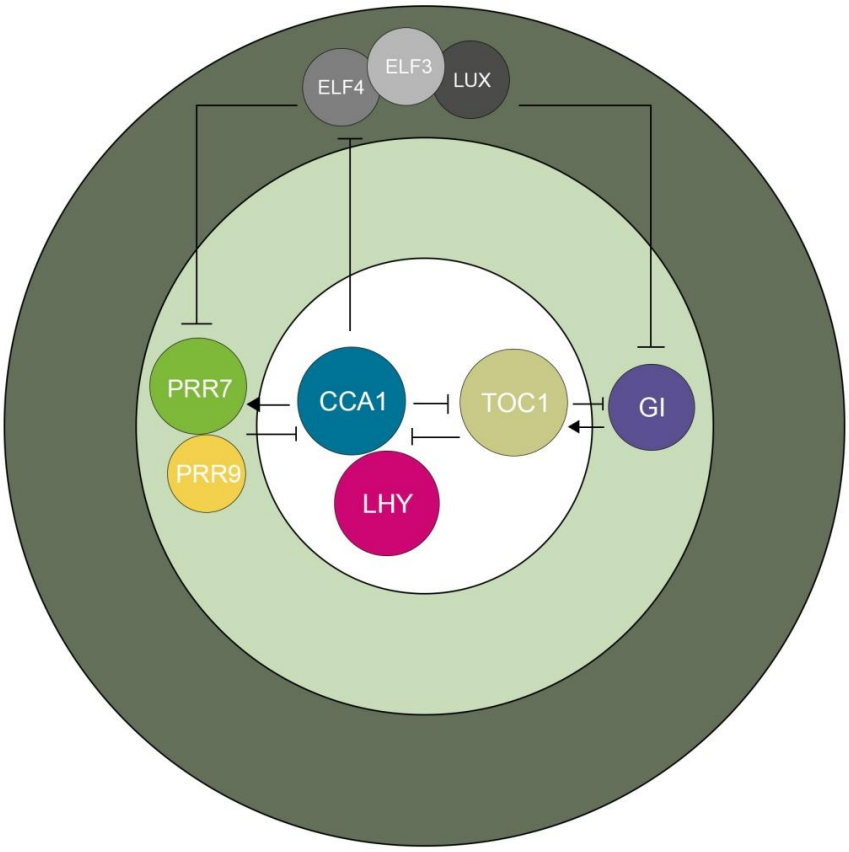

Figure 5.2 The three-layer clock model.

The three-layer clock model divides the clock into three hierarchies. The core components CCA1, LHY, and TOC1 are included in the first layer (white cycle). Defined as “adjuster”, PRR7 and PRR9 are included in the second layer (light green cycle). The third layer (dark green cycle) contains the “signal mediators”, such as ELF3

In conclusion, since many organisms have evolved a circadian clock, the clock itself should be fairly conserved. Therefore, I propose that the clock only contains two genes, a *MyB* and a *PRR*. Considering the algae, its clock may not contain a temperature-regulation pathway, due to constant temperature in water. From an evolutionary perspective, living organisms may develop temperature-regulating clock systems when they left the water and started to live on the land. This could have driven an increase in clock complexity.

5.2 Perspectives

5.2.1 Clock rhythms under different temperature

The *hsp90.2-3* mutant under warm-cold entrainment showed a longer period compared to the Ws wild type. The entrainment condition was 22°C for 12h and 16°C for 12h. The free running stage was at 22°C. To examine effect of Hsp90 on the clock at different temperature, more experiments can be performed under different entrainment conditions.

The warm entrainment condition can be set as 28°C for 12h and 22°C for 12h while the cool entrainment condition can be set as 16°C for 12h and 12°C for 12h. As the period is lengthened by higher temperature and shortened by lower temperature, but what remains unclear is how the clock behaves under these entrainment condition when Hsp90 is inhibited. There must be several temperature regulation-pathways involved in the *Arabidopsis* circadian clock, as the dynamic balance between LHY and GI at higher temperature provides temperature compensation while at lower temperatures CCA1 plays a greater role in temperature compensation and the maintenance of rhythm robustness (Gould et al., 2006). It will also be interesting to examine how *cca1*, *lhy*, *toc1*, *prr7*, *prr9*, *gi,* and *elf3* mutants respond to higher and lower temperatures when Hsp90 is inhibited.

5.2.2 Temperature effect on transcription

The mRNA accumulation data was collected from seedlings growing under normal temperature entrainment condition. This revealed how Hsp90 influenced the transcription of clock genes. However, at different temperatures, the gene accumulation of *CCA1*, *LHY*, *PRR7*, *PRR9*, and *GI* can vary, especially in darkness (Mizuno et al., 2014). Thus, it is worth testing the effect of Hsp90 on gene accumulation at different temperatures.

As demonstrated in Chapter 3, ELF3 is one target of Hsp90. Moreover, evening complex ELF3-ELF4-LUX represses the transcription of *PRR7*, *PRR9* and *GI*, but this repression was compromised by exposure to higher temperatures (Mizuno et al., 2014). However, elevated *PRR7*, *PRR9*, and *GI* mRNA accumulations were eliminated in the *elf3-1* mutant (Thines and Harmon, 2010). Examining the

accumulation of clock genes in *elf3* mutant with or without Hsp90 being inhibited may reveal how Hsp90 influence the clock through ELF3.

5.2.3 Analysis of other Hsp90.2 mutants

I measured the period of other *hsp90.2* mutants (*hsp90.2-1*, *hsp90.2-4*, *hsp90.2-6*, *hsp90.2-7,* and *hsp90.2-8*), which gave a basic insight on the clocks of these *hsp90.2* mutants. More experiments should be performed to examine the other clock properties of these *hsp90.2* mutants. These could include measuring period under cool and warm temperature, measuring phase, and examine the transcription and protein levels of the clock components.

The *hsp90.2-4* and *hsp90.2-8* mutations are more interesting, because they resulted in a short period, which is different from other *hsp90.2* mutations. However, the mechanism is still unclear. As GDA can lengthen the period, it will be interesting to test if the period shortening in *hsp90.2-4* and *hsp90.2-8* mutants can be compromised or enhanced by GDA.

In the future, it can be helpful to generate *hsp90.2 cca1*, *hsp90.2 lhy*, *hsp90.2 elf3* double mutants. These mutants can be used to identify potential targets of Hsp90.2 involved in different regulation pathways. GDA can mimic the *hsp90.2-3* mutation, as they may both result in defects of ATP-binding. However, for *hsp90.2-4* and *hsp90.2-8* mutants, they showed a shorter period. To identify how *hsp90* shortens the period, the *hsp90.2* and clock genes double mutants are required.

5.2.4 Protein assays on Hsp90.2 and clock components

As I identified in Chapter 3, ELF3 could physically interact with Hsp90 (Figure 3.13). However, the detailed mechanism needs to be further studied. It is possible that the interaction is ATP-dependent. Therefore, blocking ATP-binding may interrupt the interactions between Hsp90.2 and ELF3. Either adding GDA or removing ATP can reveal if the interaction between Hsp90 and ELF3 is ATP-dependent. By adding ATP analogues instead of ATP, the interaction may also be interrupted.

The Hsp90.2-ELF3 interaction may not only be ATP-dependent. The point mutations of *hsp90.2-4* and *hsp90.2-8* may also alter the conformation of the protein-binding sites of Hsp90.2, which may directly interrupt the interaction between Hsp90.2

and its protein clients. It is possible that the clock components bind to different site on the middle domain of Hsp90.2. Therefore, when one binding site is mutated, only some of components, but not all are influenced. In conclusion, how Hsp90 functions regulatory roles will be explored in further details using the available biochemical, genetic, and chemical tools.

Chapter 6 References

Alabadi, D., Oyama, T., Yanovsky, M.J., Harmon, F.G., Mas, P., and Kay, S.A. (2001). Reciprocal regulation between TOC1 and LHY/CCA1 within the Arabidopsis circadian clock. Science *293*, 880-883.

Ali, M.M., Roe, S.M., Vaughan, C.K., Meyer, P., Panaretou, B., Piper, P.W., Prodromou, C., and Pearl, L.H. (2006). Crystal structure of an Hsp90-nucleotide-p23/Sba1 closed chaperone complex. Nature *440*, 1013-1017.

Balasubramanian, S., Sureshkumar, S., Lempe, J., and Weigel, D. (2006). Potent induction of Arabidopsis thaliana flowering by elevated growth temperature. PLoS genetics *2*, e106.

Baudry, A., Ito, S., Song, Y.H., Strait, A.A., Kiba, T., Lu, S., Henriques, R., Pruneda-Paz, J.L., Chua, N.H., Tobin, E.M.*, et al.* (2010). F-box proteins FKF1 and LKP2 act in concert with ZEITLUPE to control Arabidopsis clock progression. The Plant cell *22*, 606-622.

Boikoglou, E., Ma, Z., von Korff, M., Davis, A.M., Nagy, F., and Davis, S.J. (2011). Environmental memory from a circadian oscillator: the Arabidopsis thaliana clock differentially integrates perception of photic vs. thermal entrainment. Genetics *189*, 655-664.

Covington, M.F., and Harmer, S.L. (2007). The circadian clock regulates auxin signaling and responses in Arabidopsis. PLoS biology *5*, e222.

Covington, M.F., Maloof, J.N., Straume, M., Kay, S.A., and Harmer, S.L. (2008). Global transcriptome analysis reveals circadian regulation of key pathways in plant growth and development. Genome biology *9*, R130.

Covington, M.F., Panda, S., Liu, X.L., Strayer, C.A., Wagner, D.R., and Kay, S.A. (2001). ELF3 modulates resetting of the circadian clock in Arabidopsis. The Plant cell *13*, 1305-1315.

Cowen, L.E. (2008). The evolution of fungal drug resistance: modulating the trajectory from genotype to phenotype. Nature reviews Microbiology *6*, 187-198.

Crawford, A.J., McLachlan, D.H., Hetherington, A.M., and Franklin, K.A. (2012). High temperature exposure increases plant cooling capacity. Current biology : CB *22*, R396-397.

David, K.M., Armbruster, U., Tama, N., and Putterill, J. (2006). Arabidopsis GIGANTEA protein is post-transcriptionally regulated by light and dark. FEBS letters *580*, 1193-1197.

Devlin, P.F., and Kay, S.A. (2000). Cryptochromes are required for phytochrome signaling to the circadian clock but not for rhythmicity. The Plant cell *12*, 2499-2510.

Dodd, A.N., Salathia, N., Hall, A., Kevei, E., Toth, R., Nagy, F., Hibberd, J.M., Millar, A.J., and Webb, A.A. (2005). Plant circadian clocks increase photosynthesis, growth, survival, and competitive advantage. Science *309*, 630-633.

Edwards, K.D., Anderson, P.E., Hall, A., Salathia, N.S., Locke, J.C., Lynn, J.R., Straume, M., Smith, J.Q., and Millar, A.J. (2006). FLOWERING LOCUS C mediates natural variation in the high-temperature response of the Arabidopsis circadian clock. The Plant cell *18*, 639-650.

Eriksson, M.E., Hanano, S., Southern, M.M., Hall, A., and Millar, A.J. (2003). Response regulator homologues have complementary, light-dependent functions in the Arabidopsis circadian clock. Planta *218*, 159-162.

Farre, E.M., Harmer, S.L., Harmon, F.G., Yanovsky, M.J., and Kay, S.A. (2005). Overlapping and distinct roles of PRR7 and PRR9 in the Arabidopsis circadian clock. Current biology : CB *15*, 47-54.

Fowler, S., Lee, K., Onouchi, H., Samach, A., Richardson, K., Morris, B., Coupland, G., and Putterill, J. (1999). GIGANTEA: a circadian clock-controlled gene that regulates photoperiodic flowering in Arabidopsis and encodes a protein with several possible membrane-spanning domains. The EMBO journal *18*, 4679-4688.

Franklin, K.A., Lee, S.H., Patel, D., Kumar, S.V., Spartz, A.K., Gu, C., Ye, S., Yu, P., Breen, G., Cohen, J.D.*, et al.* (2011). Phytochrome-interacting factor 4 (PIF4) regulates auxin biosynthesis at high temperature. Proceedings of the National Academy of Sciences of the United States of America *108*, 20231-20235.

Fujiwara, S., Wang, L., Han, L., Suh, S.S., Salome, P.A., McClung, C.R., and Somers, D.E. (2008). Post-translational regulation of the Arabidopsis circadian clock through selective proteolysis and phosphorylation of pseudo-response regulator proteins. The Journal of biological chemistry *283*, 23073-23083.

Gould, P.D., Locke, J.C., Larue, C., Southern, M.M., Davis, S.J., Hanano, S., Moyle, R., Milich, R., Putterill, J., Millar, A.J.*, et al.* (2006). The molecular basis of temperature compensation in the Arabidopsis circadian clock. The Plant cell *18*, 1177-1187.

Green, R.M., and Tobin, E.M. (1999). Loss of the circadian clock-associated protein 1 in Arabidopsis results in altered clock-regulated gene expression. Proceedings of the National Academy of Sciences of the United States of America *96*, 4176-4179.

Gutierrez, R.A., Ewing, R.M., Cherry, J.M., and Green, P.J. (2002). Identification of unstable transcripts in Arabidopsis by cDNA microarray analysis: rapid decay is associated with a group of touch- and specific clock-controlled genes. Proceedings of the National Academy of Sciences of the United States of America *99*, 11513-11518.

Hanano, S., Domagalska, M.A., Nagy, F., and Davis, S.J. (2006). Multiple phytohormones influence distinct parameters of the plant circadian clock. Genes to cells : devoted to molecular & cellular mechanisms *11*, 1381-1392.

Harmer, S.L. (2009). The circadian system in higher plants. Annual review of plant biology *60*, 357-377.

Harmer, S.L., Hogenesch, J.B., Straume, M., Chang, H.S., Han, B., Zhu, T., Wang, X., Kreps, J.A., and Kay, S.A. (2000). Orchestrated transcription of key pathways in Arabidopsis by the circadian clock. Science *290*, 2110-2113.

Heintzen, C., Nater, M., Apel, K., and Staiger, D. (1997). AtGRP7, a nuclear RNA-binding protein as a component of a circadian-regulated negative feedback loop in Arabidopsis thaliana. Proceedings of the National Academy of Sciences of the United States of America *94*, 8515-8520.

Herrero, E., Kolmos, E., Bujdoso, N., Yuan, Y., Wang, M., Berns, M.C., Uhlworm, H., Coupland, G., Saini, R., Jaskolski, M.*, et al.* (2012). EARLY FLOWERING4 recruitment of EARLY FLOWERING3 in the nucleus sustains the Arabidopsis circadian clock. The Plant cell *24*, 428-443.

Hessling, M., Richter, K., and Buchner, J. (2009). Dissection of the ATP-induced conformational cycle of the molecular chaperone Hsp90. Nature structural & molecular biology *16*, 287-293.

Highkin, H.R., and Hanson, J.B. (1954). Possible Interaction between Light-dark Cycles and Endogenous Daily Rhythms on the Growth of Tomato Plants. Plant physiology *29*, 301-302.

Hornitschek, P., Kohnen, M.V., Lorrain, S., Rougemont, J., Ljung, K., Lopez-Vidriero, I., Franco-Zorrilla, J.M., Solano, R., Trevisan, M., Pradervand, S.*, et al.* (2012). Phytochrome interacting factors 4 and 5 control seedling growth in changing light conditions by directly controlling auxin signaling. The Plant journal : for cell and molecular biology *71*, 699-711.

Horwitz, J. (1992). Alpha-crystallin can function as a molecular chaperone. Proceedings of the National Academy of Sciences of the United States of America *89*, 10449-10453.

Hubert, D.A., He, Y., McNulty, B.C., Tornero, P., and Dangl, J.L. (2009). Specific Arabidopsis HSP90.2 alleles recapitulate RAR1 cochaperone function in plant NB-LRR disease resistance protein regulation. Proceedings of the National Academy of Sciences of the United States of America *106*, 9556-9563.

Hubert, D.A., Tornero, P., Belkhadir, Y., Krishna, P., Takahashi, A., Shirasu, K., and Dangl, J.L. (2003). Cytosolic HSP90 associates with and modulates the Arabidopsis RPM1 disease resistance protein. The EMBO journal *22*, 5679-5689.

Jackson, S.E., Queitsch, C., and Toft, D. (2004). Hsp90: from structure to phenotype. Nature structural & molecular biology *11*, 1152-1155.

Jarosz, D.F., and Lindquist, S. (2010). Hsp90 and environmental stress transform the adaptive value of natural genetic variation. Science *330*, 1820-1824.

Kaczorowski, K.A., and Quail, P.H. (2003). Arabidopsis PSEUDO-RESPONSE REGULATOR7 is a signaling intermediate in phytochrome-regulated seedling deetiolation and phasing of the circadian clock. The Plant cell *15*, 2654-2665.

Kiba, T., Henriques, R., Sakakibara, H., and Chua, N.H. (2007). Targeted degradation of PSEUDO-RESPONSE REGULATOR5 by an SCFZTL complex regulates clock function and photomorphogenesis in Arabidopsis thaliana. The Plant cell *19*, 2516-2530.

Kim, J.Y., Song, H.R., Taylor, B.L., and Carre, I.A. (2003). Light-regulated translation mediates gated induction of the Arabidopsis clock protein LHY. The EMBO journal *22*, 935-944.

Kim, T.S., Kim, W.Y., Fujiwara, S., Kim, J., Cha, J.Y., Park, J.H., Lee, S.Y., and Somers, D.E. (2011). HSP90 functions in the circadian clock through stabilization of

the client F-box protein ZEITLUPE. Proceedings of the National Academy of Sciences of the United States of America *108*, 16843-16848.

Kim, W.Y., Fujiwara, S., Suh, S.S., Kim, J., Kim, Y., Han, L., David, K., Putterill, J., Nam, H.G., and Somers, D.E. (2007). ZEITLUPE is a circadian photoreceptor stabilized by GIGANTEA in blue light. Nature *449*, 356-360.

Kloppstech, K. (1985). Diurnal and circadian rhythmicity in the expression of light-induced plant nuclear messenger RNAs. Planta *165*, 502-506.

Koini, M.A., Alvey, L., Allen, T., Tilley, C.A., Harberd, N.P., Whitelam, G.C., and Franklin, K.A. (2009). High temperature-mediated adaptations in plant architecture require the bHLH transcription factor PIF4. Current biology : CB *19*, 408-413.

Kolmos, E., Herrero, E., Bujdoso, N., Millar, A.J., Toth, R., Gyula, P., Nagy, F., and Davis, S.J. (2011). A reduced-function allele reveals that EARLY FLOWERING3 repressive action on the circadian clock is modulated by phytochrome signals in Arabidopsis. The Plant cell *23*, 3230-3246.

Krukenberg, K.A., Street, T.O., Lavery, L.A., and Agard, D.A. (2011). Conformational dynamics of the molecular chaperone Hsp90. Quarterly reviews of biophysics *44*, 229-255.

Kumar, S.V., Lucyshyn, D., Jaeger, K.E., Alos, E., Alvey, E., Harberd, N.P., and Wigge, P.A. (2012). Transcription factor PIF4 controls the thermosensory activation of flowering. Nature *484*, 242-245.

Kumar, S.V., and Wigge, P.A. (2010). H2A.Z-containing nucleosomes mediate the thermosensory response in Arabidopsis. Cell *140*, 136-147.

Lidder, P., Gutierrez, R.A., Salome, P.A., McClung, C.R., and Green, P.J. (2005). Circadian control of messenger RNA stability. Association with a sequence-specific messenger RNA decay pathway. Plant physiology *138*, 2374-2385.

Lindquist, S. (1986). The heat-shock response. Annual review of biochemistry *55*, 1151-1191.

Lindquist, S., and Craig, E.A. (1988). The heat-shock proteins. Annual review of genetics *22*, 631-677.

Locke, J.C., Southern, M.M., Kozma-Bognar, L., Hibberd, V., Brown, P.E., Turner, M.S., and Millar, A.J. (2005). Extension of a genetic network model by iterative experimentation and mathematical analysis. Molecular systems biology *1*, 2005 0013.

Lohmann, C., Eggers-Schumacher, G., Wunderlich, M., and Schoffl, F. (2004). Two different heat shock transcription factors regulate immediate early expression of stress genes in Arabidopsis. Molecular genetics and genomics : MGG *271*, 11-21.

Martin-Tryon, E.L., Kreps, J.A., and Harmer, S.L. (2007). GIGANTEA acts in blue light signaling and has biochemically separable roles in circadian clock and flowering time regulation. Plant physiology *143*, 473-486.

Mas, P., Alabadi, D., Yanovsky, M.J., Oyama, T., and Kay, S.A. (2003a). Dual role of TOC1 in the control of circadian and photomorphogenic responses in Arabidopsis. The Plant cell *15*, 223-236.

Mas, P., Kim, W.Y., Somers, D.E., and Kay, S.A. (2003b). Targeted degradation of TOC1 by ZTL modulates circadian function in Arabidopsis thaliana. Nature *426*, 567-570.

Mayer, M.P. (2010). Gymnastics of molecular chaperones. Molecular cell *39*, 321-331.

McClung, C.R. (2006). Plant circadian rhythms. The Plant cell *18*, 792-803.

McClung, C.R., and Davis, S.J. (2010). Ambient thermometers in plants: from physiological outputs towards mechanisms of thermal sensing. Current biology : CB *20*, R1086-1092.

McWatters, H.G., Bastow, R.M., Hall, A., and Millar, A.J. (2000). The ELF3 zeitnehmer regulates light signalling to the circadian clock. Nature *408*, 716-720.

McWatters, H.G., Kolmos, E., Hall, A., Doyle, M.R., Amasino, R.M., Gyula, P., Nagy, F., Millar, A.J., and Davis, S.J. (2007). ELF4 is required for oscillatory properties of the circadian clock. Plant physiology *144*, 391-401.

Michael, T.P., and McClung, C.R. (2003). Enhancer trapping reveals widespread circadian clock transcriptional control in Arabidopsis. Plant physiology *132*, 629-639.

Michael, T.P., Mockler, T.C., Breton, G., McEntee, C., Byer, A., Trout, J.D., Hazen, S.P., Shen, R., Priest, H.D., Sullivan, C.M.*, et al.* (2008). Network discovery pipeline elucidates conserved time-of-day-specific cis-regulatory modules. PLoS genetics *4*, e14.

Michael, T.P., Salome, P.A., Yu, H.J., Spencer, T.R., Sharp, E.L., McPeek, M.A., Alonso, J.M., Ecker, J.R., and McClung, C.R. (2003). Enhanced fitness conferred by naturally occurring variation in the circadian clock. Science *302*, 1049-1053.

Mickler, M., Hessling, M., Ratzke, C., Buchner, J., and Hugel, T. (2009). The large conformational changes of Hsp90 are only weakly coupled to ATP hydrolysis. Nature structural & molecular biology *16*, 281-286.

Milioni, D., and Hatzopoulos, P. (1997). Genomic organization of hsp90 gene family in Arabidopsis. Plant molecular biology *35*, 955-961.

Millar, A.J., Short, S.R., Chua, N.H., and Kay, S.A. (1992). A novel circadian phenotype based on firefly luciferase expression in transgenic plants. The Plant cell *4*, 1075-1087.

Millar, A.J., Straume, M., Chory, J., Chua, N.H., and Kay, S.A. (1995). The regulation of circadian period by phototransduction pathways in Arabidopsis. Science *267*, 1163-1166.

Mizoguchi, T., Wheatley, K., Hanzawa, Y., Wright, L., Mizoguchi, M., Song, H.R., Carre, I.A., and Coupland, G. (2002). LHY and CCA1 are partially redundant genes required to maintain circadian rhythms in Arabidopsis. Developmental cell *2*, 629-641.

Mizuno, T., Nomoto, Y., Oka, H., Kitayama, M., Takeuchi, A., Tsubouchi, M., and Yamashino, T. (2014). Ambient temperature signal feeds into the circadian clock transcriptional circuitry through the EC nighttime repressor in Arabidopsis thaliana. Plant & cell physiology.

Mockaitis, K., and Estelle, M. (2008). Auxin receptors and plant development: a new signaling paradigm. Annual review of cell and developmental biology *24*, 55-80.

Nakamichi, N., Kiba, T., Henriques, R., Mizuno, T., Chua, N.H., and Sakakibara, H. (2010). PSEUDO-RESPONSE REGULATORS 9, 7, and 5 are transcriptional repressors in the Arabidopsis circadian clock. The Plant cell *22*, 594-605.

Nakamichi, N., Kita, M., Ito, S., Sato, E., Yamashino, T., and Mizuno, T. (2005). The Arabidopsis pseudo-response regulators, PRR5 and PRR7, coordinately play essential roles for circadian clock function. Plant & cell physiology *46*, 609-619.

Nishizawa-Yokoi, A., Tainaka, H., Yoshida, E., Tamoi, M., Yabuta, Y., and Shigeoka, S. (2010). The 26S proteasome function and Hsp90 activity involved in the regulation of HsfA2 expression in response to oxidative stress. Plant & cell physiology *51*, 486-496.

Onai, K., Okamoto, K., Nishimoto, H., Morioka, C., Hirano, M., Kami-Ike, N., and Ishiura, M. (2004). Large-scale screening of Arabidopsis circadian clock mutants by a high-throughput real-time bioluminescence monitoring system. The Plant journal : for cell and molecular biology *40*, 1-11.

Ouyang, Y., Andersson, C.R., Kondo, T., Golden, S.S., and Johnson, C.H. (1998). Resonating circadian clocks enhance fitness in cyanobacteria. Proceedings of the National Academy of Sciences of the United States of America *95*, 8660-8664.

Park, D.H., Somers, D.E., Kim, Y.S., Choy, Y.H., Lim, H.K., Soh, M.S., Kim, H.J., Kay, S.A., and Nam, H.G. (1999). Control of circadian rhythms and photoperiodic flowering by the Arabidopsis GIGANTEA gene. Science *285*, 1579-1582.

Pearl, L.H., and Prodromou, C. (2006). Structure and mechanism of the Hsp90 molecular chaperone machinery. Annual review of biochemistry *75*, 271-294.

Picard, D. (2002). Heat-shock protein 90, a chaperone for folding and regulation. Cellular and molecular life sciences : CMLS *59*, 1640-1648.

Portoles, S., and Mas, P. (2010). The functional interplay between protein kinase CK2 and CCA1 transcriptional activity is essential for clock temperature compensation in Arabidopsis. PLoS genetics *6*, e1001201.

Prasinos, C., Krampis, K., Samakovli, D., and Hatzopoulos, P. (2005). Tight regulation of expression of two Arabidopsis cytosolic Hsp90 genes during embryo development. Journal of experimental botany *56*, 633-644.

Pratt, W.B., Galigniana, M.D., Harrell, J.M., and DeFranco, D.B. (2004). Role of hsp90 and the hsp90-binding immunophilins in signalling protein movement. Cellular signalling *16*, 857-872.

Proveniers, M.C., and van Zanten, M. (2013). High temperature acclimation through PIF4 signaling. Trends in plant science *18*, 59-64.

Queitsch, C., Sangster, T.A., and Lindquist, S. (2002). Hsp90 as a capacitor of phenotypic variation. Nature *417*, 618-624.

Rizhsky, L., Liang, H., and Mittler, R. (2002). The combined effect of drought stress and heat shock on gene expression in tobacco. Plant physiology *130*, 1143-1151.

Romero, I., Fuertes, A., Benito, M.J., Malpica, J.M., Leyva, A., and Paz-Ares, J. (1998). More than 80R2R3-MYB regulatory genes in the genome of Arabidopsis thaliana. The Plant journal : for cell and molecular biology *14*, 273-284.

Saibil, H. (2013). Chaperone machines for protein folding, unfolding and disaggregation. Nature reviews Molecular cell biology *14*, 630-642.

Salome, P.A., and McClung, C.R. (2005). PSEUDO-RESPONSE REGULATOR 7 and 9 are partially redundant genes essential for the temperature responsiveness of the Arabidopsis circadian clock. The Plant cell *17*, 791-803.

Salome, P.A., Weigel, D., and McClung, C.R. (2010). The role of the Arabidopsis morning loop components CCA1, LHY, PRR7, and PRR9 in temperature compensation. The Plant cell *22*, 3650-3661.

Samach, A., and Wigge, P.A. (2005). Ambient temperature perception in plants. Current opinion in plant biology *8*, 483-486.

Sangster, T.A., and Queitsch, C. (2005). The HSP90 chaperone complex, an emerging force in plant development and phenotypic plasticity. Current opinion in plant biology *8*, 86-92.

Sangster, T.A., Salathia, N., Lee, H.N., Watanabe, E., Schellenberg, K., Morneau, K., Wang, H., Undurraga, S., Queitsch, C., and Lindquist, S. (2008a). HSP90-buffered genetic variation is common in Arabidopsis thaliana. Proceedings of the National Academy of Sciences of the United States of America *105*, 2969-2974.

Sangster, T.A., Salathia, N., Undurraga, S., Milo, R., Schellenberg, K., Lindquist, S., and Queitsch, C. (2008b). HSP90 affects the expression of genetic variation and developmental stability in quantitative traits. Proceedings of the National Academy of Sciences of the United States of America *105*, 2963-2968.

Schaffer, R., Landgraf, J., Accerbi, M., Simon, V., Larson, M., and Wisman, E. (2001). Microarray analysis of diurnal and circadian-regulated genes in Arabidopsis. The Plant cell *13*, 113-123.

Schaffer, R., Ramsay, N., Samach, A., Corden, S., Putterill, J., Carre, I.A., and Coupland, G. (1998). The late elongated hypocotyl mutation of Arabidopsis disrupts circadian rhythms and the photoperiodic control of flowering. Cell *93*, 1219-1229.

Schomburg, F.M., Patton, D.A., Meinke, D.W., and Amasino, R.M. (2001). FPA, a gene involved in floral induction in Arabidopsis, encodes a protein containing RNA-recognition motifs. The Plant cell *13*, 1427-1436.

Schoning, J.C., Streitner, C., Page, D.R., Hennig, S., Uchida, K., Wolf, E., Furuya, M., and Staiger, D. (2007). Auto-regulation of the circadian slave oscillator component AtGRP7 and regulation of its targets is impaired by a single RNA recognition motif point mutation. The Plant journal : for cell and molecular biology *52*, 1119-1130.

Scroggins, B.T., Robzyk, K., Wang, D., Marcu, M.G., Tsutsumi, S., Beebe, K., Cotter, R.J., Felts, S., Toft, D., Karnitz, L.*, et al.* (2007). An acetylation site in the middle domain of Hsp90 regulates chaperone function. Molecular cell *25*, 151-159.

Shinozaki, F., Minami, M., Chiba, T., Suzuki, M., Yoshimatsu, K., Ichikawa, Y., Terasawa, K., Emori, Y., Matsumoto, K., Kurosaki, T.*, et al.* (2006). Depletion of

hsp90beta induces multiple defects in B cell receptor signaling. The Journal of biological chemistry *281*, 16361-16369.

Shirasu, K., and Schulze-Lefert, P. (2003). Complex formation, promiscuity and multi-functionality: protein interactions in disease-resistance pathways. Trends in plant science *8*, 252-258.

Somers, D.E., Devlin, P.F., and Kay, S.A. (1998a). Phytochromes and cryptochromes in the entrainment of the Arabidopsis circadian clock. Science *282*, 1488-1490.

Somers, D.E., Schultz, T.F., Milnamow, M., and Kay, S.A. (2000). ZEITLUPE encodes a novel clock-associated PAS protein from Arabidopsis. Cell *101*, 319-329.

Somers, D.E., Webb, A.A., Pearson, M., and Kay, S.A. (1998b). The short-period mutant, toc1-1, alters circadian clock regulation of multiple outputs throughout development in Arabidopsis thaliana. Development *125*, 485-494.

Southern, M.M., and Millar, A.J. (2005). Circadian genetics in the model higher plant, Arabidopsis thaliana. Methods in enzymology *393*, 23-35.

Stavang, J.A., Gallego-Bartolome, J., Gomez, M.D., Yoshida, S., Asami, T., Olsen, J.E., Garcia-Martinez, J.L., Alabadi, D., and Blazquez, M.A. (2009). Hormonal regulation of temperature-induced growth in Arabidopsis. The Plant journal : for cell and molecular biology *60*, 589-601.

Strayer, C., Oyama, T., Schultz, T.F., Raman, R., Somers, D.E., Mas, P., Panda, S., Kreps, J.A., and Kay, S.A. (2000). Cloning of the Arabidopsis clock gene TOC1, an autoregulatory response regulator homolog. Science *289*, 768-771.

Sun, J., Qi, L., Li, Y., Chu, J., and Li, C. (2012). PIF4-mediated activation of YUCCA8 expression integrates temperature into the auxin pathway in regulating arabidopsis hypocotyl growth. PLoS genetics *8*, e1002594.

Terasawa, K., Minami, M., and Minami, Y. (2005). Constantly updated knowledge of Hsp90. Journal of biochemistry *137*, 443-447.

Thines, B., and Harmon, F.G. (2010). Ambient temperature response establishes ELF3 as a required component of the core Arabidopsis circadian clock. Proceedings of the National Academy of Sciences of the United States of America *107*, 3257-3262.

Untergasser, A., Nijveen, H., Rao, X., Bisseling, T., Geurts, R., and Leunissen, J.A. (2007). Primer3Plus, an enhanced web interface to Primer3. Nucleic acids research *35*, W71-74.

van Zanten, M., Voesenek, L.A., Peeters, A.J., and Millenaar, F.F. (2009). Hormone- and light-mediated regulation of heat-induced differential petiole growth in Arabidopsis. Plant physiology *151*, 1446-1458.

Voinnet, O., Rivas, S., Mestre, P., and Baulcombe, D. (2003). An enhanced transient expression system in plants based on suppression of gene silencing by the p19 protein of tomato bushy stunt virus. The Plant journal : for cell and molecular biology *33*, 949-956.

Wang, W., Barnaby, J.Y., Tada, Y., Li, H., Tor, M., Caldelari, D., Lee, D.U., Fu, X.D., and Dong, X. (2011). Timing of plant immune responses by a central circadian regulator. Nature *470*, 110-114.

Wang, Z.Y., and Tobin, E.M. (1998). Constitutive expression of the CIRCADIAN CLOCK ASSOCIATED 1 (CCA1) gene disrupts circadian rhythms and suppresses its own expression. Cell *93*, 1207-1217.

Wayne, N., Mishra, P., and Bolon, D.N. (2011). Hsp90 and client protein maturation. Methods in molecular biology *787*, 33-44.

Wegele, H., Muller, L., and Buchner, J. (2004). Hsp70 and Hsp90--a relay team for protein folding. Reviews of physiology, biochemistry and pharmacology *151*, 1-44.

Weigel, D., and Jurgens, G. (2002). Stem cells that make stems. Nature *415*, 751-754.

Whitesell, L., Shifrin, S.D., Schwab, G., and Neckers, L.M. (1992). Benzoquinonoid ansamycins possess selective tumoricidal activity unrelated to src kinase inhibition. Cancer research *52*, 1721-1728.

Woelfle, M.A., Ouyang, Y., Phanvijhitsiri, K., and Johnson, C.H. (2004). The adaptive value of circadian clocks: an experimental assessment in cyanobacteria. Current biology : CB *14*, 1481-1486.

Yakir, E., Hilman, D., Harir, Y., and Green, R.M. (2007). Regulation of output from the plant circadian clock. The FEBS journal *274*, 335-345.

Yamada, K., Fukao, Y., Hayashi, M., Fukazawa, M., Suzuki, I., and Nishimura, M. (2007). Cytosolic HSP90 regulates the heat shock response that is responsible for heat acclimation in Arabidopsis thaliana. The Journal of biological chemistry *282*, 37794-37804.

Yamamoto, Y., Sato, E., Shimizu, T., Nakamich, N., Sato, S., Kato, T., Tabata, S., Nagatani, A., Yamashino, T., and Mizuno, T. (2003). Comparative genetic studies on the APRR5 and APRR7 genes belonging to the APRR1/TOC1 quintet implicated in circadian rhythm, control of flowering time, and early photomorphogenesis. Plant & cell physiology *44*, 1119-1130.

Young, J.C., Moarefi, I., and Hartl, F.U. (2001). Hsp90: a specialized but essential protein-folding tool. The Journal of cell biology *154*, 267-273.

Zuehlke, A., and Johnson, J.L. (2010). Hsp90 and co-chaperones twist the functions of diverse client proteins. Biopolymers *93*, 211-217.

Acknowledgments

This thesis reflects my effort in the Davis' group for the last three and a half years. First of all, I would like to gratefully and sincerely thank my supervisor, Prof. Dr. Seth J. Davis, for his guidance, understanding, tolerance, and patience during my PhD training. He encouraged me to not only grow as an experimentalist but also as an independent thinker. For me, he is the best supervisor ever. Honestly speaking, I am not an outstanding student. Time to time, I felt so sorry for not fully devoting myself to making considerable progress in my research work. I really appreciate the opportunity to develop my own individuality. For everything you've done for me, Prof. Dr. Seth J. Davis, I thank you.

Thanks to Amanda Davis for her collaboration, support, and her invaluable contribution to keep the Davis lab running.

Thanks to Takayuki Shindo for his technical guidance, generous sharing of his perfect plasmid constructs, and routine conversations on "*One Piece*" and "US Non-farm Payrolls"

Thanks to Jieun for her cool protocols, her nice advice on my experiments, and her own experiences in making better performance.

Thanks to the rest of Davis lab former and current members for their contribution to a nice environment in the Davis lab.

Thanks to Quan Wang for his kind help and delicious dinners during those four months when my kitchen was under repair.

Thanks to the administration and personnel offices, and scientific service groups for their expertise and patience.

In addition, I am thankful to Prof. Dr. Dorothea Bartels for being my internal supervisor and the reviewer of my thesis. And thanks to Prof. Dr. Peter Dörmann and Prof. Dr. Frank Hochholdinger for being my defense committee members.

Finally, and most importantly, I would like to thank my parents for endlessly loving me, showing faith in me, and giving me liberty to choose what I desired.